



**Australian Government**  
**Department of Agriculture, Fisheries and Forestry**

# Technical Report

**Program and KPI:** Sub-program 1.2 KPI 3.11

**Report Title:** Standardised methodology for sampling and image analysis, and validation resource data for CT as the calibrating standard for lean meat yield measurement

**Prepared by:** K. Mata, C.G. Jose, A. Williams & G.E. Gardner  
Murdoch University

**Date published:** 1 October 2021



# Final report

---

## Effect of machine and carcass factors on CT prediction of carcass composition in Lamb and Beef

Project code: V.TEC.1714  
Prepared by: K. Mata, C.G. Jose, A. Williams & G.E. Gardner  
Murdoch University  
Date published: 09/06/2021

PUBLISHED BY  
Meat & Livestock Australia Limited  
PO Box 1961  
NORTH SYDNEY NSW 2059

Meat & Livestock Australia acknowledges the matching funds provided by the Australian Government to support the research and development detailed in this publication.

This publication is published by Meat & Livestock Australia Limited ABN 39 081 678 364 (MLA). Care is taken to ensure the accuracy of the information contained in this publication. However MLA cannot accept responsibility for the accuracy or completeness of the information or opinions contained in the publication. You should make your own enquiries before making decisions concerning your interests. Reproduction in whole or in part of this publication is prohibited without prior written consent of MLA.

## Executive summary

To support computed tomography (CT) as the reference method for measuring lean meat yield within the Australian beef and lamb industry, it is important to understand the robustness of this measure, and the factors that can influence its estimate of carcass composition. This work was undertaken through a series of experiments that established the immediate repeatability of CT estimates of carcass composition, the impact of changes to scanning methodology such as carcass sectioning and freeze/thaw protocols, and the effect of machine scanning voltage and CT scan slice width. This work demonstrated several outcomes:

1. CT estimates of carcass composition are almost perfectly repeatable.
2. Carcass sectioning has a small impact on CT estimates of carcass composition, so we propose a standardized carcass sectioning method for lamb to be used when CT is used as the reference standard for calibrating other measurement technologies.
3. CT scan slice width has a small impact on CT estimates of carcass composition, so we propose 5mm slice widths as the standard method for lamb to be used when CT is used as the reference standard for calibrating other measurement technologies.
4. CT scan voltage has a substantial impact on CT estimates of carcass composition, so we propose that a standardized voltage of 120kV is applied for beef when CT is used as the reference standard for calibrating other measurement technologies. Scans captured at other voltages can be corrected to give the 120kV equivalent estimate of carcass composition, but for consistency this should be avoided for calibration purposes.
5. Scanning beef butts in a frozen state decreases tissue Hounsfield unit values, particularly for fat and lean tissues, resulting in substantial variation in their estimated composition within beef butts. Alternatively, scanning these same sections after they have thawed produces values very similar to those scanned fresh, implying that carcasses can be frozen and then defrosted prior to CT scanning and still deliver consistent results.
6. When the CT methodology is standardised, it demonstrates substantially better repeatability than determining carcass composition using chemical methods.
7. CT scanning plastic phantoms has demonstrated that the values reported across a range of plastics of different densities only vary slightly between scans and machines. These small variations are likely to be readily accounted for through scanning common calibrating phantoms like the XTE-CT test piece.

# Table of contents

<b>1. Background .....</b>	<b>7</b>
<b>2. Project Objectives .....</b>	<b>7</b>
<b>3. The repeatability of CT scanning in Lamb .....</b>	<b>7</b>
<b>3.1 Methodology.....</b>	<b>8</b>
3.1.1 Experiment 1- Effect of CT voltage and immediate repeatability in lamb.....	8
3.1.1.1 Carcase Selection .....	8
3.1.1.2 CT Scanning .....	8
3.1.1.3 Image Analysis of 120kV scans.....	9
3.1.1.4 Image analysis of 100kV and 135kV scans.....	9
3.1.1.5 Statistical analysis .....	10
3.1.2 Experiment 2 – Effect of CT scan slice width on composition estimates.....	11
3.1.2.1 Carcase Selection .....	11
3.1.2.2 Ct Scanning and Image analysis .....	12
3.1.2.3 Experiment 2 Statistical analysis.....	12
3.1.3 Experiment 3 – Lamb Chemical Composition.....	13
3.1.3.1 Carcase Selection .....	13
3.1.3.2 CT scanning and Image analysis.....	13
3.1.3.3 Chemical composition sampling .....	14
3.1.3.4 Chemical composition analysis .....	14
3.1.3.5 Statistical Analysis.....	15
<b>3.2 Results.....</b>	<b>16</b>
3.2.1 The effect of carcase sectioning on CT composition.....	16
3.2.1 Chemical composition .....	32
3.2.1.1 Sampling variability .....	34
<b>3.3 Discussion.....</b>	<b>35</b>
3.3.1 Immediate Repeatability .....	35
3.3.2 Cut vs Whole.....	35
3.3.3 Slice Width .....	37
3.3.4 Voltage.....	37

3.3.5	Chemical composition of lamb .....	37
<b>3.4</b>	<b>Conclusions .....</b>	<b>38</b>
<b>4.</b>	<b>The repeatability of CT scanning in Beef.....</b>	<b>39</b>
<b>4.1</b>	<b>Methodology.....</b>	<b>39</b>
4.1.1	Experiment 1- bone-in short loin and rib sets.....	39
4.1.1.1	Carcase Selection .....	39
4.1.1.2	CT scanning .....	39
4.1.1.3	Image analysis.....	40
4.1.1.4	Statistical analysis .....	40
4.1.2	Experiment 2- Beef butts and Aitch bone .....	41
4.1.2.1	Carcase selection .....	41
4.1.2.2	CT scanning .....	41
4.1.2.3	Image analysis.....	42
4.1.2.4	Statistical analysis .....	42
4.1.3	Beef Chemical composition .....	43
4.1.3.1	Carcase selection .....	43
4.1.3.2	CT scanning .....	43
4.1.3.3	Image analysis.....	43
4.1.3.4	Chemical composition sampling .....	43
4.1.3.5	Chemical composition analysis .....	44
4.1.3.6	Statistical analysis .....	44
<b>4.2</b>	<b>Results.....</b>	<b>45</b>
4.2.1	Slice Width .....	45
4.2.2	Freeze/Thaw comparison .....	47
4.2.2.1	Rib sets.....	47
4.2.2.2	Short loin.....	49
4.2.3	Voltage.....	51
4.2.4	Thresholding Adjustment- fixed density and new thresholds from linear equation.....	52
4.2.5	Chemical composition of Beef.....	56
4.2.5.1	Sampling variability- Beef .....	57
<b>4.3</b>	<b>Discussion.....</b>	<b>58</b>

4.3.1	Slice Width .....	58
4.3.2	Voltage.....	58
4.3.3	Freeze/thaw effects.....	59
4.3.4	Chemical Composition .....	59
<b>4.4</b>	<b>Conclusions .....</b>	<b>59</b>
<b>5.</b>	<b>The repeatability of CT scanning plastic phantoms .....</b>	<b>61</b>
<b>5.1</b>	<b>Methodology.....</b>	<b>61</b>
5.1.1	Experiment 1- Comparison of Plastic block between different CT devices .....	61
5.1.2	Experiment 2 – Compariosn of the XTE-CT phantom between different CT devices .....	61
<b>5.2</b>	<b>Results.....</b>	<b>63</b>
<b>5.3</b>	<b>Discussion.....</b>	<b>66</b>
<b>6.</b>	<b>References .....</b>	<b>68</b>

## **1. Background**

From March 2020 through to December 2020 multiple experiments were carried out at Murdoch University analysing the effect of various machine factors and carcass factors on CT determination of lamb and beef carcass composition. The initial experimentation in lamb investigated the effect of Voltage change on CT carcass composition prediction. Factors such as changes in slice width, the immediate repeatability of CT and the effect of sectioning a carcass on CT carcass prediction were also assessed.

Further experimentation in beef assessed the impact of slice width on CT beef carcass composition prediction while also assessing the impact of freezing and thawing on those CT predictions. The second experiment focused on the effect of voltage on CT composition predictions.

All experiments were carried out using carcass sections to allow for scanning using human medical-grade CT scanners, with concurrent analysis of plastic phantoms of known densities. The experimentation aims to solidify CT as the gold standard measure of carcass composition in the red meat industry.

When establishing CT scanning as the gold standard in predicting carcass composition, it is important to understand the outputs of different CT scanning devices. Since historical CT datasets are derived from different locations and devices around Australia, this work will clarify how the Hounsfield units (HU) vary between devices. Therefore, an additional aim of this study was to CT scan a plastic phantom of known and varying density across 3 different CT devices, to quantify the magnitude of differences in HU outputs from different devices.

## **2. Project Objectives**

Delivery of a robust system for the calibration and collection of lean meat yield data for training prediction devices.

1. Design calibration phantom that will be the gold standard for LMY prediction.
2. Affirm repeatability of scanning and calculate chemical composition to validate results on lamb.
3. Affirm repeatability of scanning and calculate chemical composition to validate results on beef.

## **3. The repeatability of CT scanning in Lamb**

## 3.1 Methodology

### 3.1.1 Experiment 1- Effect of CT voltage and immediate repeatability in lamb

Experiment 1 determined the impact of carcass sectioning and scan voltage on the bone%, lean% and fat% estimated from CT. It also assessed the immediate repeatability of these estimates.

#### 3.1.1.1 Carcass Selection

20 Lambs were selected from the MLA Katanning resource flock with known phenotypic data including hot carcass weight (HSCW) with a mean and standard deviation of 21.2kg ( $\pm$  4.07kg) and Grade rule measurement (GR) with a mean of 19.9mm ( $\pm$  6.87mm) (see **Figure 1**). Following slaughter, the lamb carcasses were maintained at 5°C until CT scanning 36 hours post-mortem.

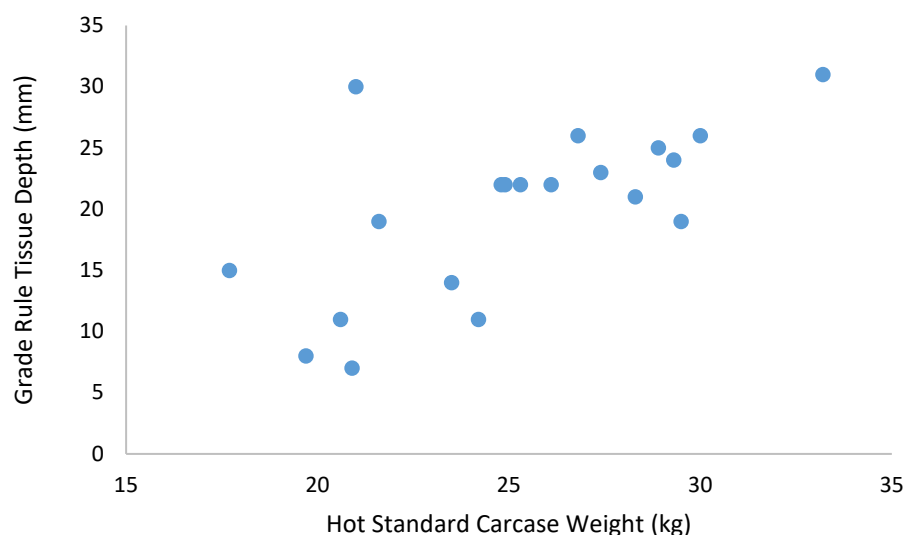


**Figure 1** - Experiment 1 carcass selection, grade rule tissue depth vs hot standard carcass weight.

#### 3.1.1.2 CT Scanning

Carcasses were CT scanned using a Canon Aquilon Lightning medical CT scanner. For all scans, the spiral abdomen protocol was selected using an acquisition slice width of 1mm and also reconstructed to 10mm slice widths. Pilot scan length of 1450 to 1780 mm depending on carcass size, field of view set at 500 mm, mA 100, revs 65, pitch 1.5 and standard algorithm.

Each carcass was first scanned whole at 120KV and then cut into fore, mid and hind sections. The fore-section was separated from the mid-section by a cut between the fourth and fifth rib. The hind-section was separated from the mid-section by a cut through the mid-length of



the sixth lumbar vertebrae. Each carcass section was weighed, and all cut sections were re-scanned in rapid succession at 100kV, 135kV, and then three times at 120kV. The three consecutive scans at 120kV enabled us to assess the immediate repeatability of this method. During consecutive scans of carcass sections, the fore, mid and hind sections were not moved until all 5 scanning protocols were complete. See **Figure 3** for Lamb section positioning in both Experiment 1 and 2.

Plastic phantoms with known densities were also scanned at 120KV before, during and after the carcasses.

### 3.1.1.3 Image Analysis of 120kV scans

For all scans captured at 120kV, The Raw DICOM images were analysed using ImageJ software (version 1.52a, National Institutes of Health, Bethesda, MD, USA in combination with Microsoft excel). Carcass images were categorized into bone, lean and fat and all non carcass portions of the image were removed. The allocation of pixels to a certain tissue type was based on fixed thresholding where fat was defined as voxels at -250 to 2.5HU, Lean muscle at 2.6-165HU and Bone at >165HU. Volume estimation was calculated using the Cavalieri stereological method illustrated in the following equation. (Gundersen, Bendtsen, Korbo, Marcussen, & Møller, 1988; Gundersen & Jensen, 1987)

$$\text{Volume}_{\text{Cav}} = d \times \sum_{g=1}^m \text{area}_g - t \times \text{area}_{\text{max}}$$

Where m represents the quantity of CT scans taken, d is the slice width(10mm), t representing the thickness of the slice (slice width)  $\text{area}_{\text{max}}$  represents the maximum area of all scans taken.

Mass was then calculated for each tissue type by averaging the HU of all pixels within each component, converting to voxel mass based upon a linear density transformation (Mull, 1984), and then multiplying by the number of voxels for that tissue type. This allowed the calculation of the weight (kg) of each tissue type (bone, lean and fat), which was then expressed as a percentage of total carcass weight at the time of CT scanning. (Anderson, 2017)

### 3.1.1.4 Image analysis of 100kV and 135kV scans

The image analysis of scans captured at 100kV and 135kV was undertaken in two ways. Firstly, the same method described above for the scans captured at 120kV was applied to the 100kV and 135kV scans. Secondly, these scans were re-analysed using a separate set of thresholds to allocate voxels to bone, lean and fat components. To determine these thresholds a single cross-sectional image from the fore-limb region of each carcass was

selected within the 120kV scans. Within this image 3 regions of interest consisting of at least 50 pixels were identified anatomically to consist of bone, lean, and fat tissue, and their average Hounsfield unit value calculated. These same voxels were then matched to those in the corresponding scans taken at 100kV and 135 kV, to determine the average Hounsfield unit value for these same pixels at 100kV and 135kV. This process was repeated for each carcass, producing 20 separate estimates of average Hounsfield unit value for bone, lean, and fat tissue at voltages of 100, 120, and 135kV, a total of 180 separate values. A conversion equation was then established enabling the transformation of HU values from those scanned at 120kV into their 100 or 135kV equivalent values. For the bone average Hounsfield unit value, firstly estimates taken at 100kV were regressed against those taken at 120kV, and then secondly estimates taken at 135kV were regressed against those taken at 120kV. This process was repeated for the fat and lean values, establishing transformation equations (see **Figure 17**) which were then applied to the threshold values set at 120kV enabling conversion of the thresholds into their 100 or 135kV equivalent values which are shown in **Table 1**. These new threshold values were then applied to the scans captured at 100kV and 135kV, using the same image analysis method described in section 2.1.3 above. The only difference was that rather than applying the Mull linear transformation (Mull, 1984) to convert to density(kg/L) and mass estimation, fixed values of tissue density were applied instead. The voxels allocated as bone were multiplied by a fixed density of  $1.43\text{g/cm}^3$ , lean by  $1.078\text{g/cm}^3$ , and fat by  $0.94\text{g/cm}^3$ . (reference)

### 3.1.1.5 Statistical analysis

The effect of carcass sectioning was assessed in the first instance using a GLM, where CT fat % estimated from sectioned carcasses were used as the dependent variable, and CT fat % estimated from whole carcasses were tested as the independent variable. The slope of this relationship, the bias estimated at the mean of the CT fat% values, the RMSE and the  $R^2$  were reported to indicate the alignment of these estimates. Secondly, the difference between the CT fat% values estimated from sectioned carcasses and whole carcasses were calculated, and then regressed against the CT fat % estimated from whole carcasses to test for any significant deviation from zero along this continuum. This process was repeated for CT lean% estimates and CT bone% estimates. Lastly, the sum of the estimated mass of the bone, muscle, and fat components for the sectioned carcass and the whole carcass were compared. The mass estimated from the sectioned components were regressed against the mass from the whole and the slope of this relationship, the bias estimated at the mean of the summed component weights, the RMSE and the  $R^2$  were reported to indicate the alignment of these estimates. Secondly, the difference between the sum of the estimated mass of the bone, muscle, and fat components for the sectioned carcass and the whole carcass were calculated, and then regressed against the whole carcass estimated mass to test for any significant deviation from zero along this continuum.

To analyse the immediate repeatability of CT scan estimates of composition, for each carcass the 3 CT fat% values estimated at 120kV were expressed as a deviation from their mean. These values were pooled, and the mean and standard deviation calculated. In addition, these values were regressed against the average CT fat % of all three scans to test for any significant deviation from zero along this continuum. In addition, the CT fat% values for the 2<sup>nd</sup> and 3<sup>rd</sup> scans were regressed against the 1<sup>st</sup> scan, and the slope of this relationship, the bias estimated at the mean of the CT fat% values, the RMSE and the R<sup>2</sup> were reported to indicate the alignment of these estimates. This process was repeated for CT lean% estimates and CT bone% estimates.

To analyse the effect of voltage on CT scan estimates of composition, for each carcass the 3 CT fat% values estimated at 120kV were expressed as a deviation from their mean. These values were pooled, and the mean and standard deviation calculated. In addition, these values were regressed against the average CT fat % of all three scans to test for any significant deviation from zero along this continuum. In addition, the CT fat% values for the 2<sup>nd</sup> and 3<sup>rd</sup> scans were regressed against the 1<sup>st</sup> scan, and the slope of this relationship, the bias estimated at the mean of the CT fat% values, the RMSE and the R<sup>2</sup> were reported to indicate the alignment of these estimates. This process was repeated for CT lean% estimates and CT bone% estimates.

### **3.1.2 Experiment 2 – Effect of CT scan slice width on composition estimates**

Experiment 2 determined the impact of scan slice width on the bone%, lean% and fat% estimated from CT.

#### **3.1.2.1 Carcass Selection**

30 lambs from Frewstall in Victoria were selected across a broad phenotypic range with a mean hot standard carcass weight (HSCW) of 22.9±3.42kg and mean GR tissue depth of 12.7±5.25kg (**Figure 2**). Following slaughter, the lamb carcasses were maintained at 5°C until CT scanning 36 hours post-mortem.

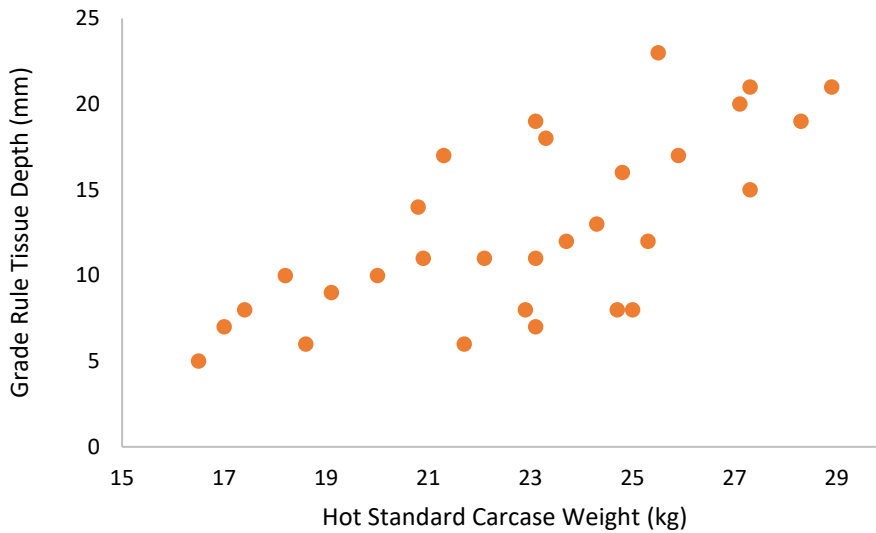


**Figure 2-** Experiment 2 Carcass Selection, Grade Rule tissue depth vs Hot Standard Carcass Weight.

### 3.1.2.2 Ct Scanning and Image analysis

Carcasses were CT scanned using a Canon Aquilion Lightning machine with Pilot scan length 1500mm, Dynamic mAs with set min/max parameter of 50 to 300mAs, FOV 500mm, rotation 0.75secs, Pitch factor 0.813, Helical pitch 65, Voltage 120kV. Images were captured at a 1mm slice width and also reconstructed into 5mm slice widths.

Image analysis was undertaken using the same protocols as described in section 2.1.3 above, using the thresholds specified for 120kV listed in **Table 1**.



**Figure 3-**Medical CT scanning of a lamb fore section, saddle and hind section.

### 3.1.2.3 Experiment 2 Statistical analysis

The effect of slice width was assessed in the first instance using a GLM, where CT fat % estimated from slice widths of 1mm were used as the dependent variable, and CT fat % estimated from slice widths of 5mm were tested as the independent variable. The slope of this relationship, the bias estimated at the mean of the CT fat% values, the RMSE and the R<sup>2</sup> were reported to indicate the alignment of these estimates. Secondly, the difference between the CT fat% values estimated at 1mm and 5 mm were calculated, and then regressed against the CT fat % estimated at 5 mm to test for any significant deviation from zero along this continuum.

### 3.1.3 Experiment 3 – Lamb Chemical Composition

#### 3.1.3.1 Carcase Selection

30 Lambs were selected from the slaughter floor during routine processing at the Frewstal abattoir in Stawell, Victoria, in February 2021. A wide range of animal weights were selected with a mean Hot Standard Carcase Weight (HSCW) of 24.7±6.47kg and mean GR tissue depth 14.3±8.05mm.

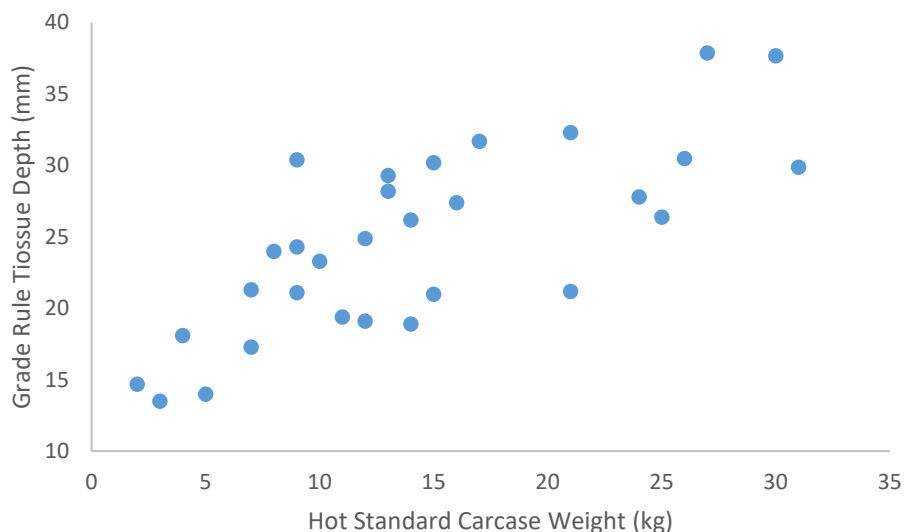


Figure 4-Experiment 3-Carcase Selection - Hot Standard Carcase Weight (kg) vs Grade Tissue Depth (mm)

#### 3.1.3.2 CT scanning and Image analysis

The carcasses were sectioned into primals (fore, saddle, hind as described in Section 2.1.2) then transported to Melbourne for scanning by a Rapiscan CT machine. Post-scanning they were transported by refrigerated logistics to Murdoch University. Carcasses were weighed on

arrival in their 3 primal sections on the day of scanning, and the saddle section was then further split at the 12/13<sup>th</sup> rib for ease of CT imaging. The lamb fore sections ranged from 7.7kg to 12.4kg, averaging 8.35kg ( $\pm 2.08$ ); the saddle section ranged from 3.6kg to 13.1kg, averaging 7.52kg ( $\pm 2.38$ ), and the hind section ranged from 4.9kg to 12.5kg with a mean weight of 8.54kg ( $\pm 1.99$ ).

Carcases were CT scanned using a Canon Aquilon Lightning machine with Pilot scan length 1500mm, Dynamic mAs with set min/max parameter of 50 to 300mAs, FOV 500mm, rotation 0.75secs, Pitch factor 0.813, Helical pitch 65, Voltage 120kV. Images were captured at a 1mm slice width and also reconstructed into 5mm slice widths.

Image analysis was undertaken using the same protocols as described in section 3.1.1.3 above, using the thresholds specified for 120kV listed in **Table 1**.

Phantoms of known density including the XTE-CT Phantom, were scanned before, during and after the 30 lamb carcasses to assess for any drift in Hounsfield units over the day.

### **3.1.3.3 Chemical composition sampling**

On completion of CT scanning, carcasses remained in their separate primal sections and were further reduced in size with the aid of a bandsaw to enable grinding in a commercial grade mincing machine. All bones were included in the end product. Any loss of mince/bone on the bandsaw was recorded by weight and the overall weight of the minced product recorded post grind. Ice was utilized as needed for ease of mincing with any addition of ice weighed to enable moisture tracking throughout.

The sectioned primals were first passed twice through a large mincing plate with holes of 35mm diameter, then again twice through a plate with holes of 5mm until a uniform and homogenous mix was created, this was then manually mixed again prior to sampling. 5 sub samples of approximately 50g wet weight were taken into plastic lidded tubes for each primal section, so a total of 15 samples per carcass and 5 per primal. (approx. 750g total weight sampled per carcass) and an additional 500g of minced product was vacuum packed in the case of being needed for further sampling.

### **3.1.3.4 Chemical composition analysis**

The individual samples were weighed wet, then freeze dried for 10 days in a commercial freeze drier, Dry matter (DM) weights were recorded and sub-sample mincing into a fine

powder was performed for better homogenization and ease of chemical analysis, this protocol did break down the bone particles well.

5g DM samples were taken from each tube (total of 450 samples) for protein analysis at an external lab with a further 5 g DM needed for ash content analysis and a further 8g DM for Soxhlet/NIR analysis for lipid.

A Protein analysis technique was used to determine total nitrogen which was then converted to its protein equivalent mass using a protein conversion factor of 6.25.

Lipid was analysed using near infrared spectroscopy (NIR) calibrated against Soxhlet fat extraction. An initial 90 samples (the first sub-sample of each carcass at each section) underwent measurement using both Soxhlet and NIR. These values were then used to train the NIR equation, with these samples differing from the routine IMF equation due to the inclusion of bone in the mixture. This equation was then applied to all other samples processed using the NIR for their prediction.

Ashing was carried out using a 600C furnace. All samples were weighed post oven-drying and prior to entering the 600C furnace. The ash extracted from the furnace was weighed and expressed relative to its sub-sample weight to determine the ash content of the entire carcass.

### **3.1.3.5 Statistical Analysis**

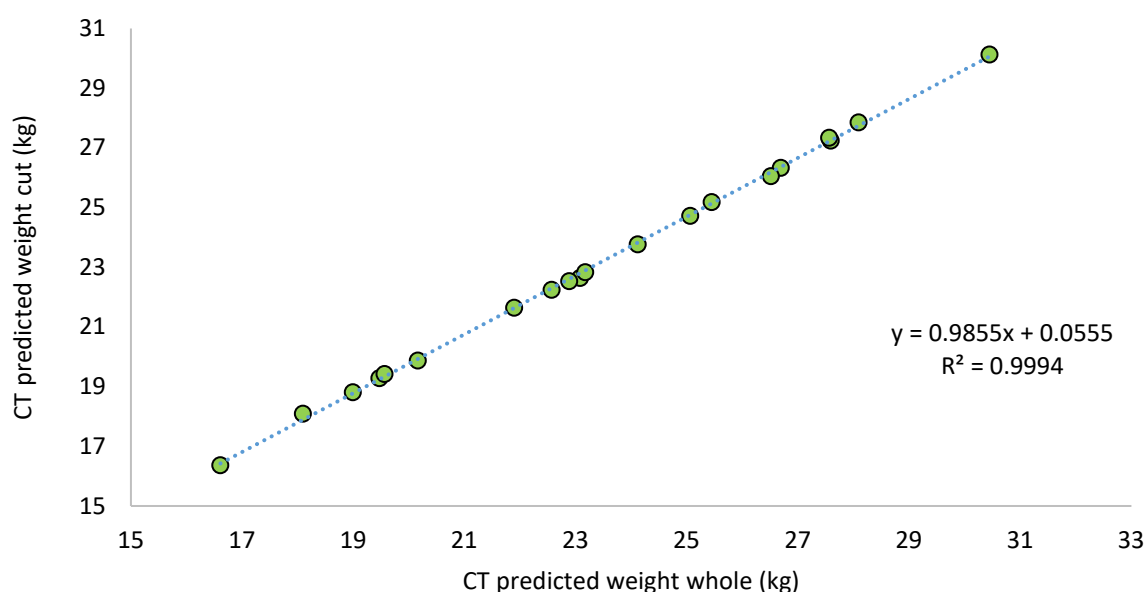
General linear modelling was used with Chemical Protein % as the dependent variable and CT lean % as the independent variable. The slope of this relationship, the bias estimated at the mean of the Chemical protein % values, the RMSE and the  $R^2$  were reported to indicate the alignment of these estimates. This was repeated for Chemical Lipid % vs CT fat %.

## 3.2 Results

### 3.2.1 The effect of carcass sectioning on CT composition

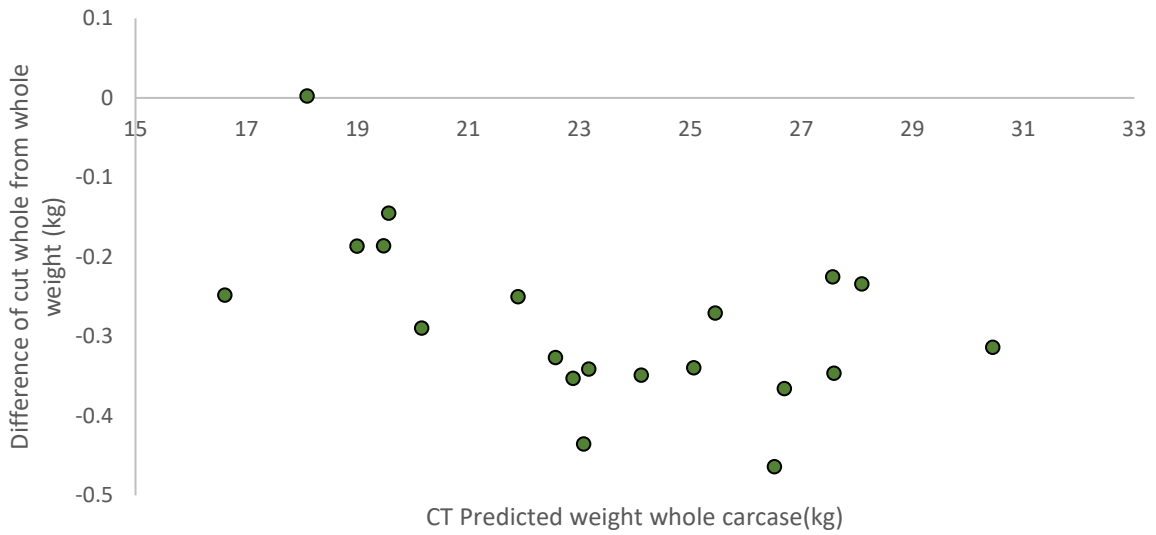
There was a strong association between the CT predicted weight of the whole carcase versus the sectioned carcase, with an  $R^2$  close to 1 (**Figure 4**). The difference in these values was on average  $-0.28\text{g}$  ( $\pm 0.106\text{g}$ ) and ranged between  $-0.46\text{g}$  and  $0.002\text{g}$ , with these differences independent of carcase weight (**Figure 5**)

When the individual percentage predictions of fat, lean and bone were compared they demonstrated a strong association with  $R^2$  values all in excess of 0.99 but showed small differences in absolute values **Figure 6**. When carcasses were sectioned the CT Fat% values were about 0.85% units higher, with this difference varying on average by 1% at the lower values and diminishing to 0.7% units higher at the higher CT fat% values (**Figure 6a**). By contrast, for sectioned carcasses the CT Lean% values were about 0.75% units lower, with this difference varying by 0.5% at the lower CT lean% values and 1% lower at the higher CT lean% values (**Figure 6b**). The differences in CT bone% values were much smaller, showing little difference at the low CT bone% values, and 0.15% units lower at the high CT bone% values (**Figure 6c**).

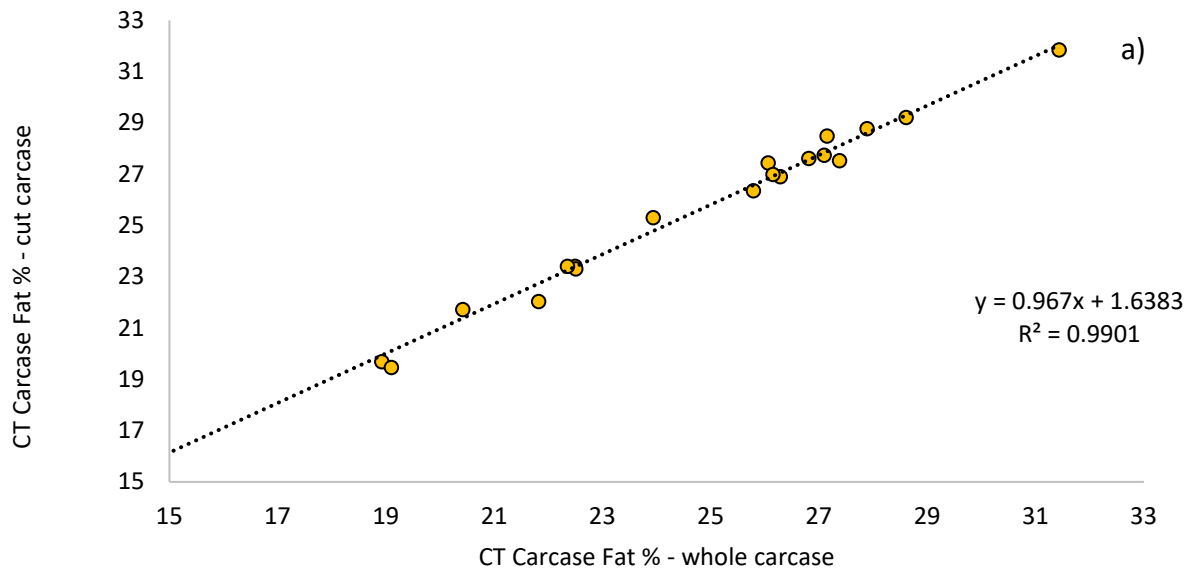


**Figure 5-** CT predicted carcage weight (kg) estimated from the sum of the bone, lean and fat components of sectioned carcasses (cut) vs whole carcasses.

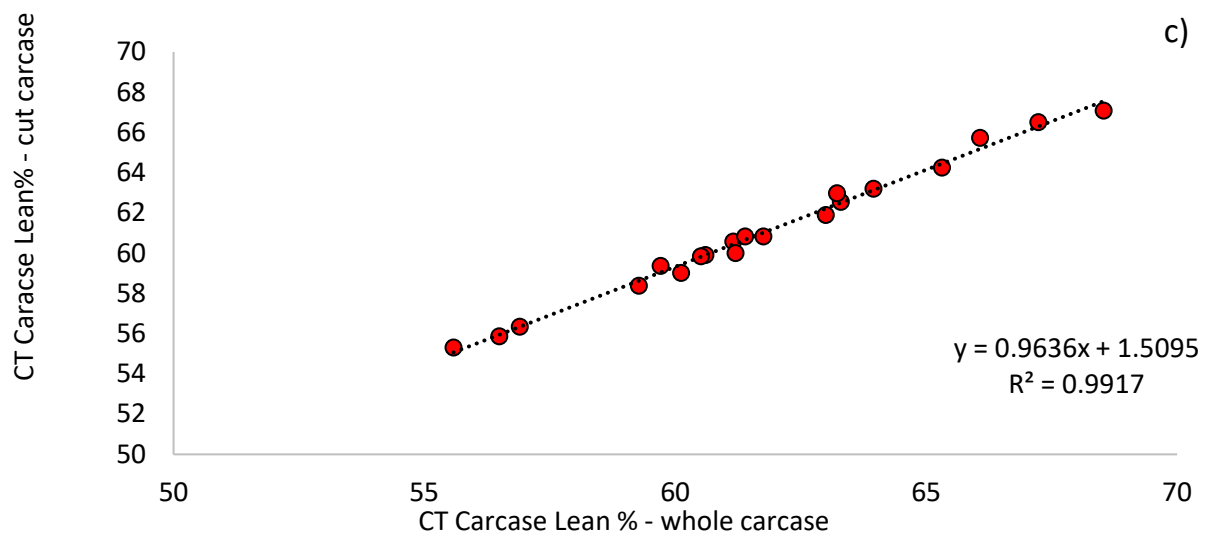
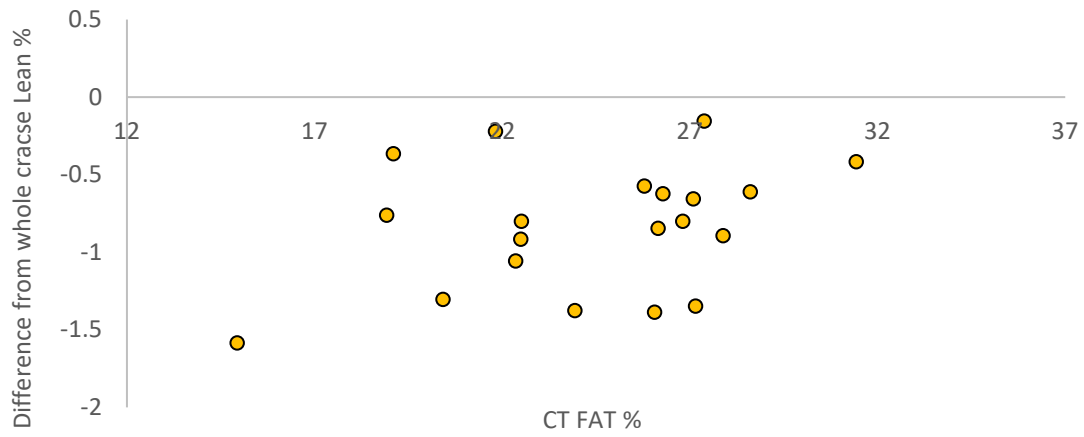


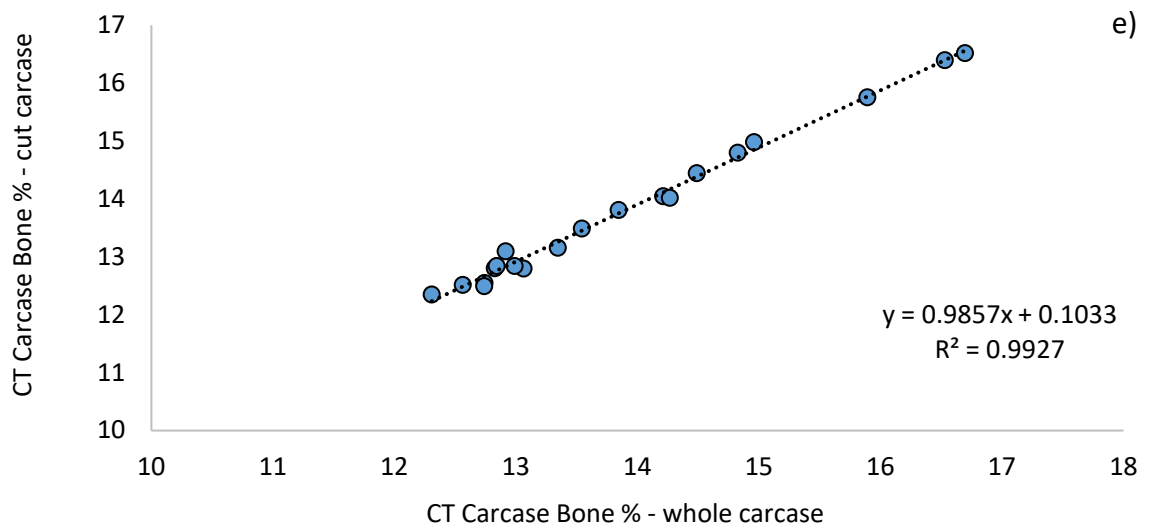
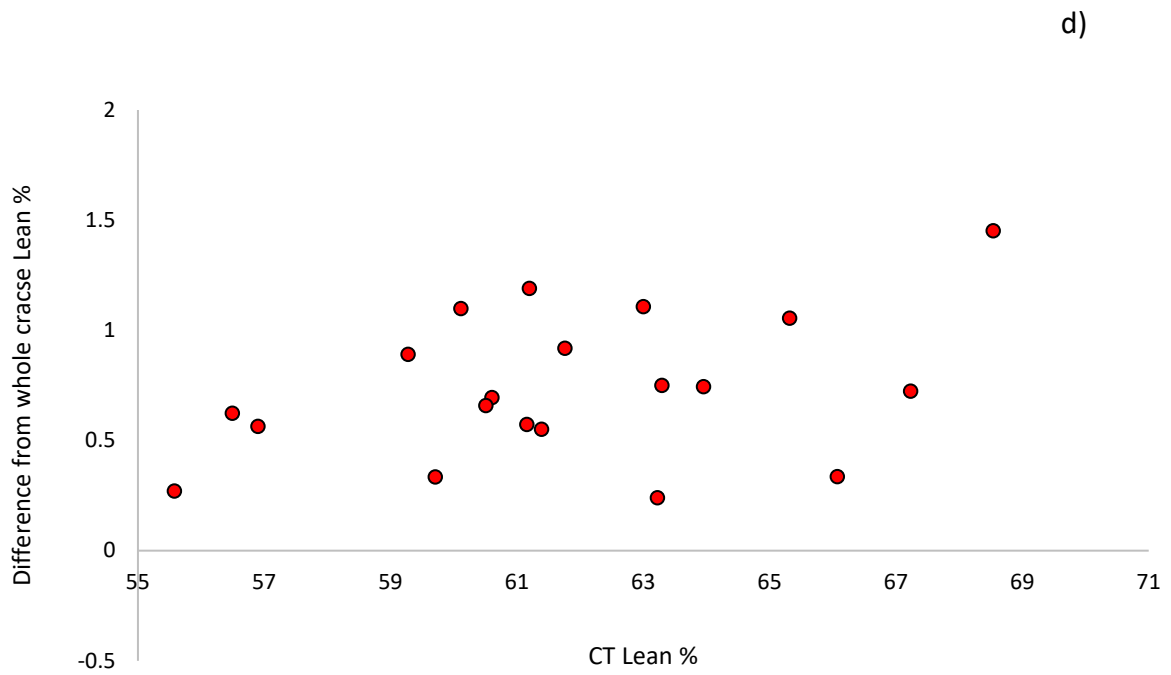


**Figure 6-** Differences of CT predicted weights of cut carcasses from CT predicted weights of whole carcasses (kg)



b)





f)

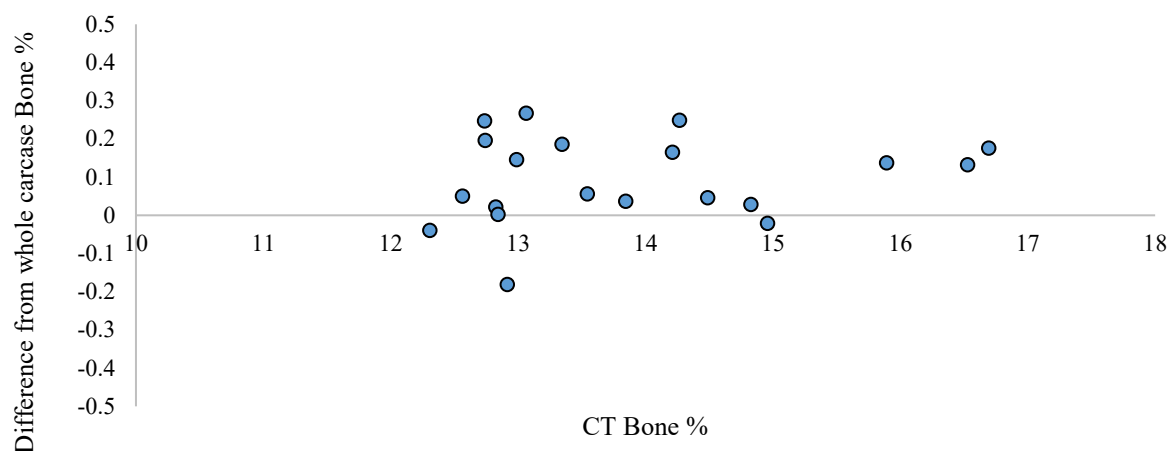


**Figure 7-**CT % Yield by tissue type of cut vs whole carcasses **a)** Fat, **c)** Lean, **d)** Bone and differences of Yield % predictions for cut vs whole carcasses by tissue type **b)** Fat, **d)** Lean and **f)** Bone

### 3.2 Immediate Repeatability

The immediate repeatability of composition prediction of a cut carcass across 3 scans at a single voltage of 120kV showed extremely high precision when predicting carcass weight with an  $R^2$  of 1 (**Figure 7-a**). Very small differences were noted from the CT predicted weight of Scan 1 for both Scan 2 and Scan 3, with both Scan 2 and Scan 3 showing an identical mean difference of -0.0049kg ( $\pm 0.005186$ ) and a maximum difference of 0.003kg and minimum of 0.018kg (**Figure 7-b**). Composition prediction based on tissue type also showed high precision with Fat % showing an  $R^2$  of 0.99 (**Figure 8 – a**), Lean % with an  $R^2$  of 0.99 (**Figure 9-a**) and lastly Bone % with an  $R^2$  of 0.99 (**Figure 10-a**). The maximum difference between the 3 scans for each carcass was less than 0.05% for Fat (**Figure 8-b**), less than 0.05% for Lean (**Figure 9-b**) and less than 0.02% for Bone (**Figure 10-b**). General Linear modelling found no consistent sources of bias between the three scans at 120kV.

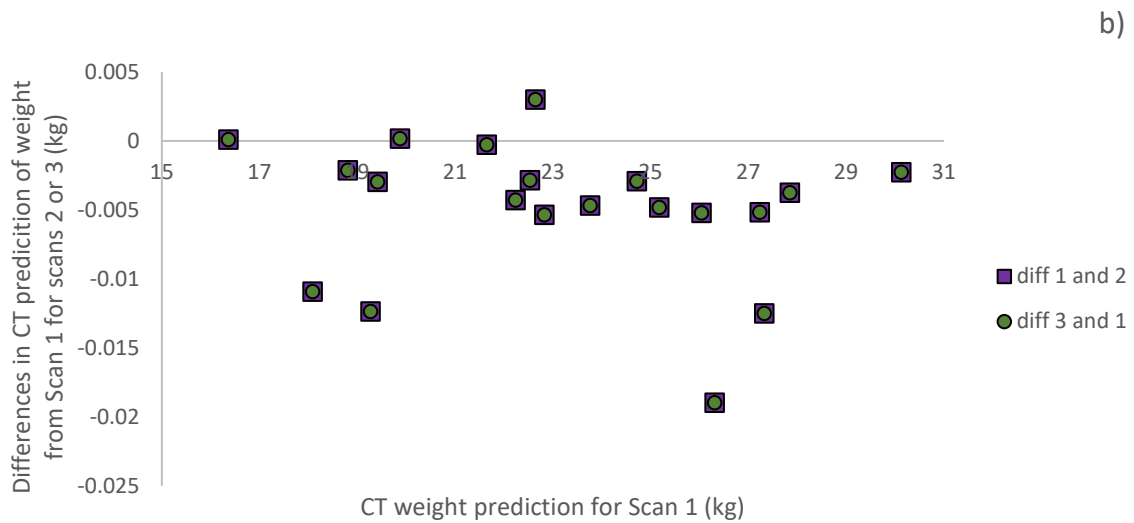
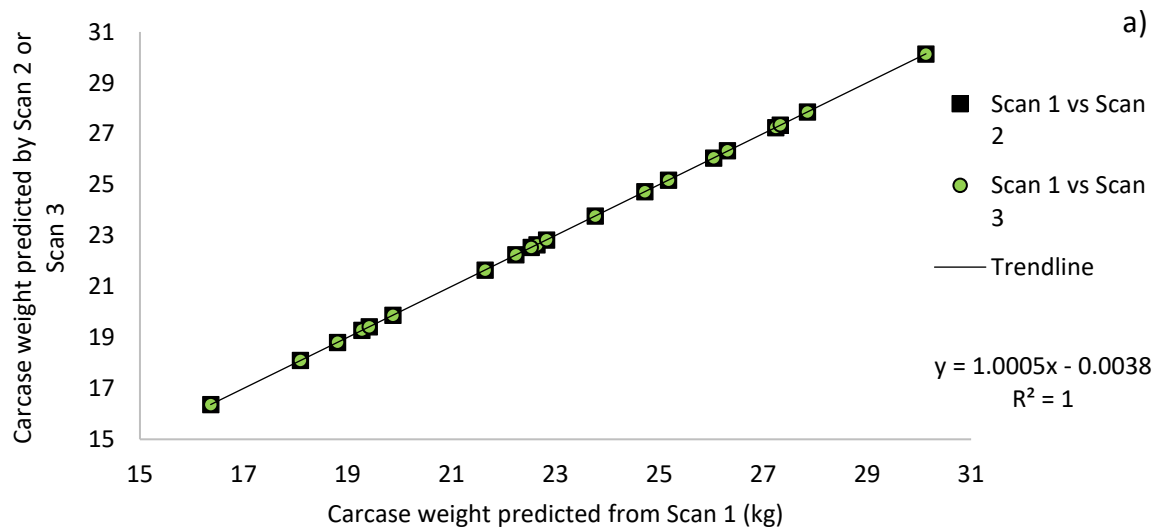


**Figure 8-** Immediate Repeatability of CT predicted carcass weight across all 3 scans a) Differences in CT weight prediction of scan 2 and 3 when compared to Scan 1, b) .

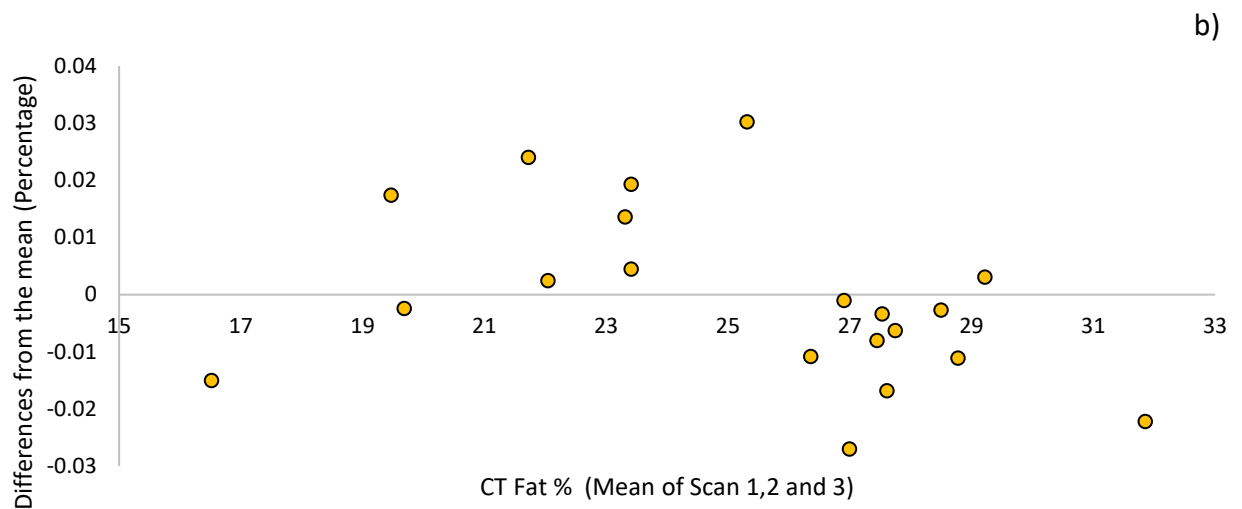
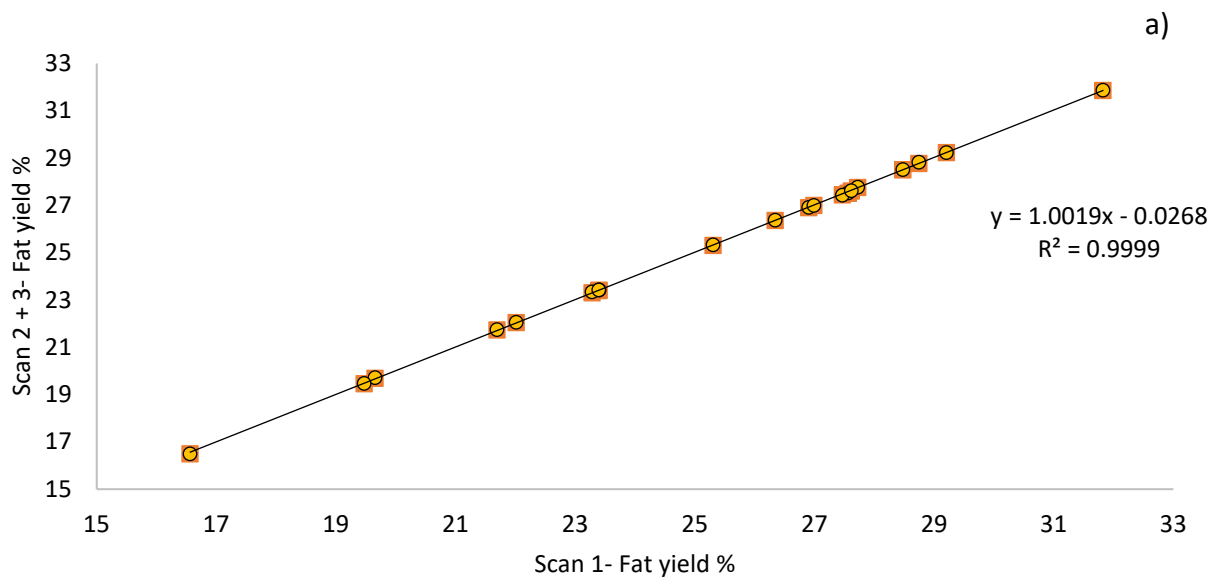


**Figure 9-a)** Repeatability for CT prediction for Fat yield %, **b)** Variation in repeatability of CT prediction of Fat Yield % (difference from the mean)

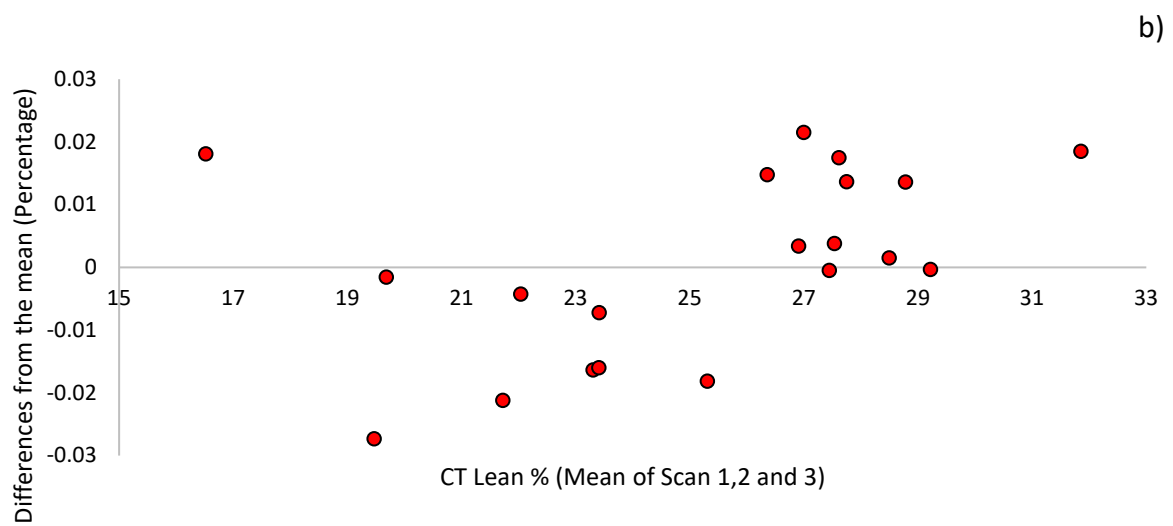
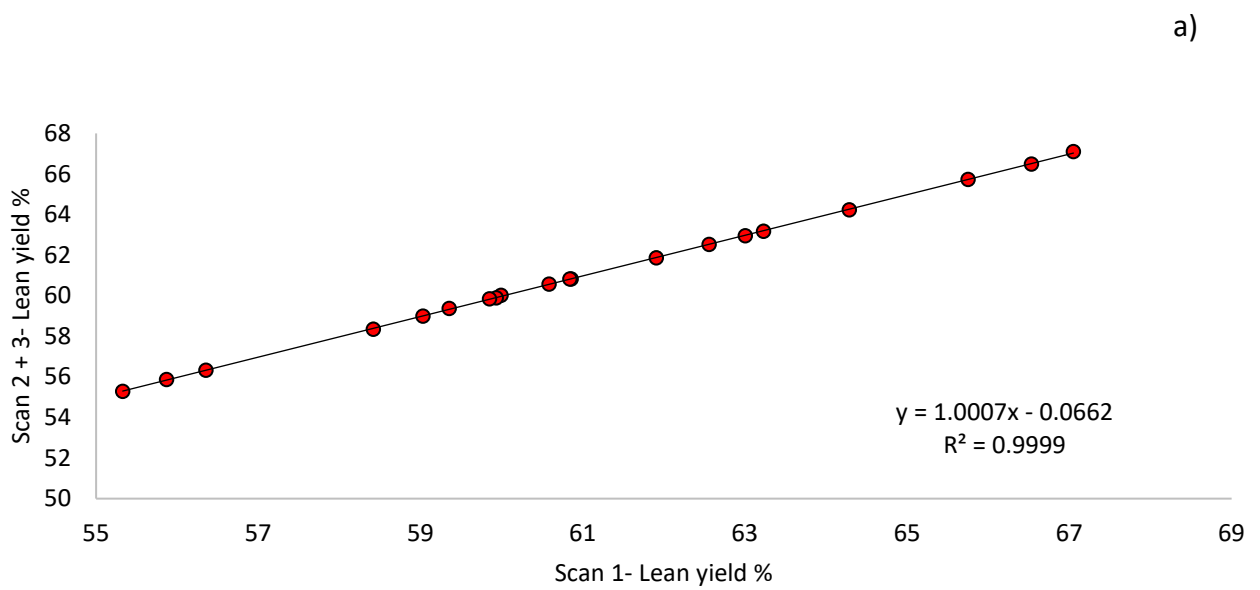


**Figure 10- a)** Repeatability for CT prediction of Lean Yield %, **b)** variation in repeatability of CT prediction of Lean Yield % (difference from the mean)

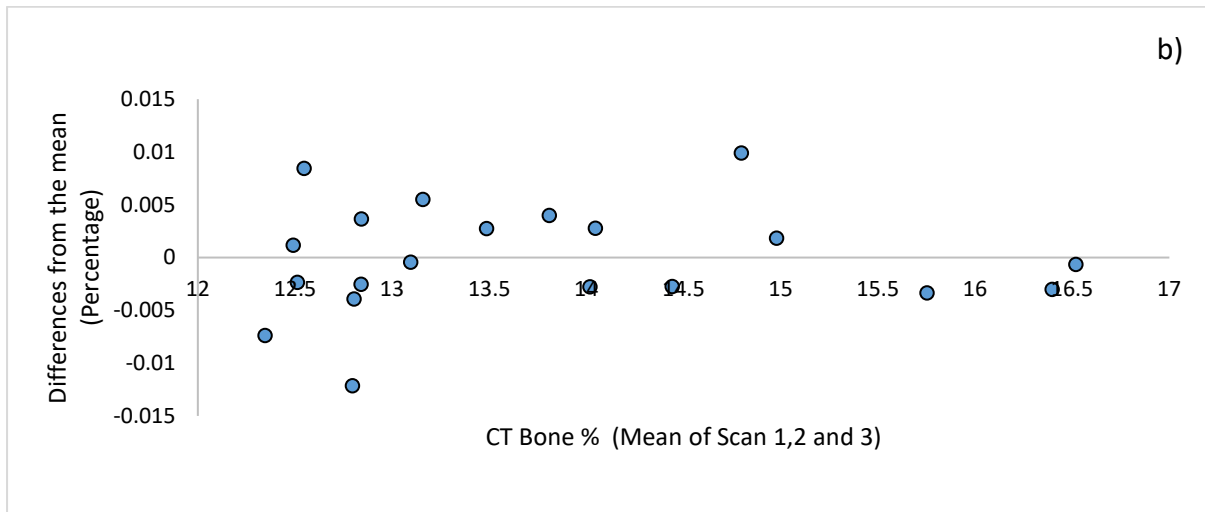
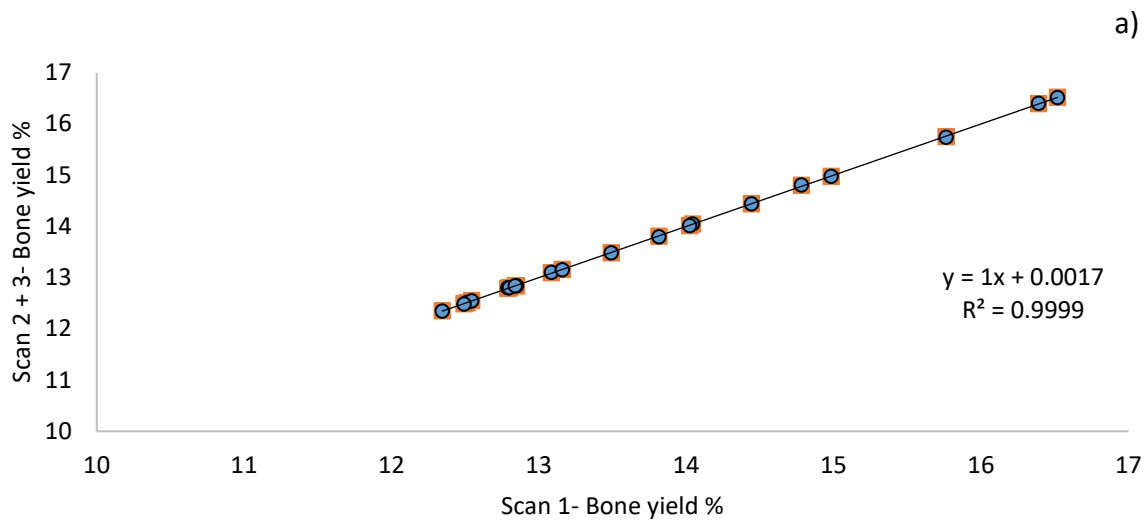
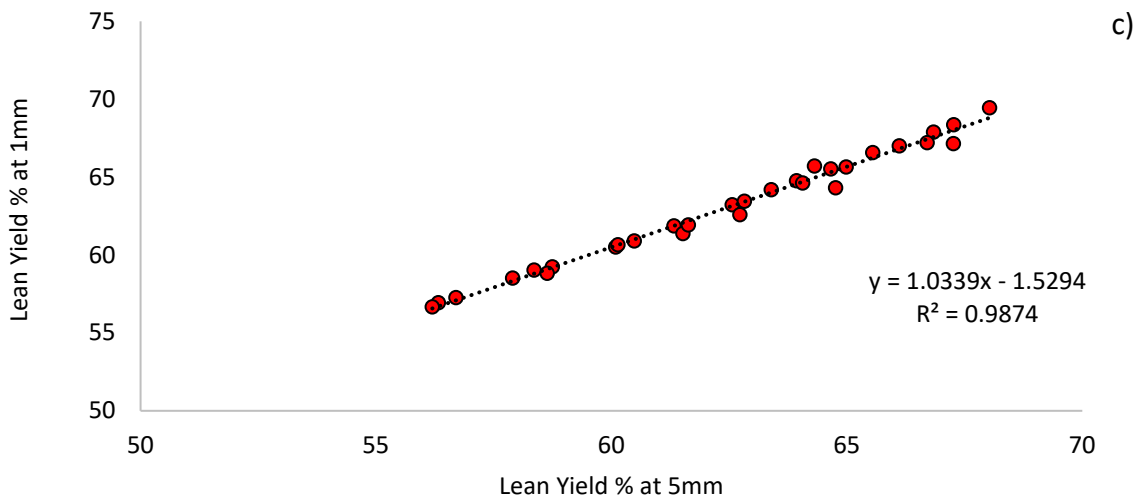
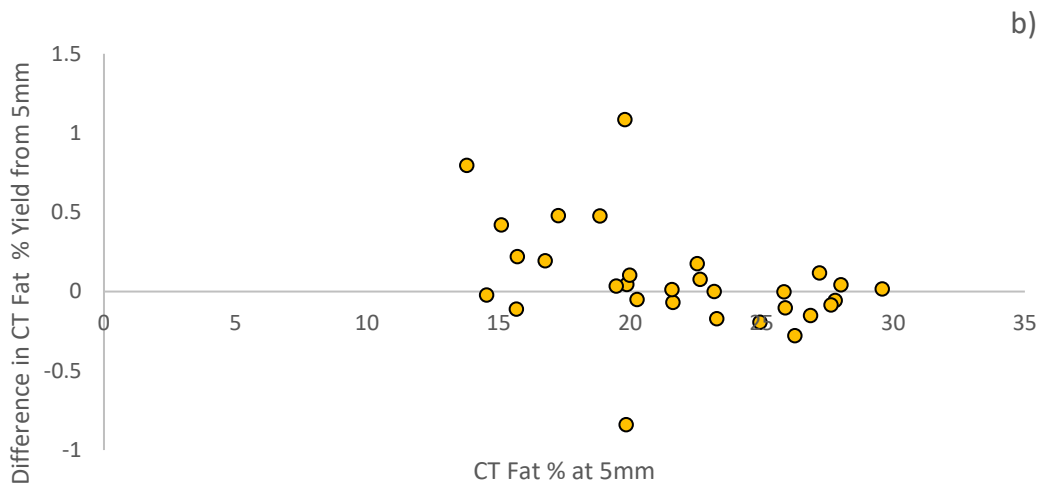
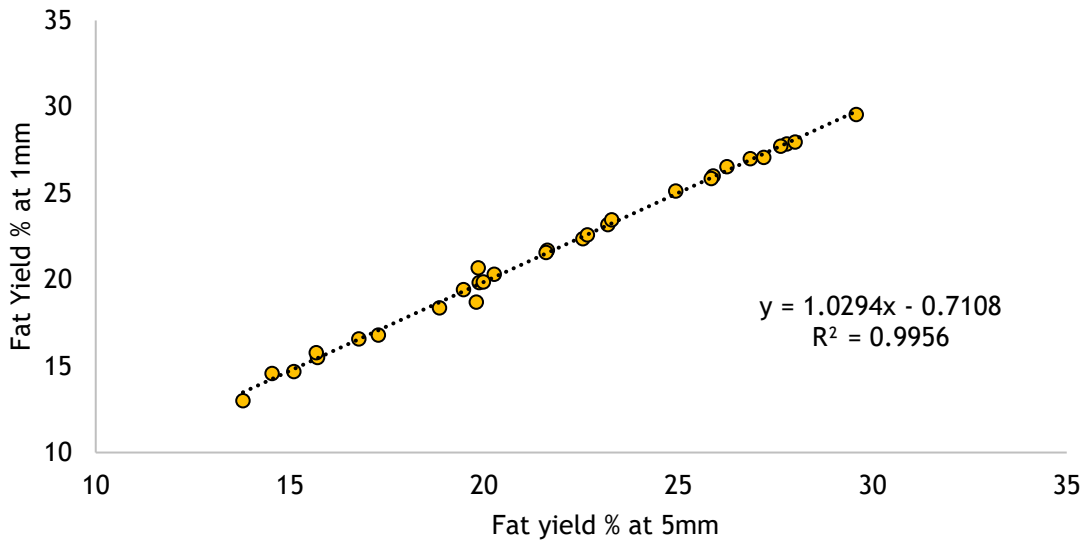


**Figure 11-a)** Repeatability for CT prediction of Bone Yield % **b)** variation in repeatability of CT prediction of Bone Yield % (difference from the mean)

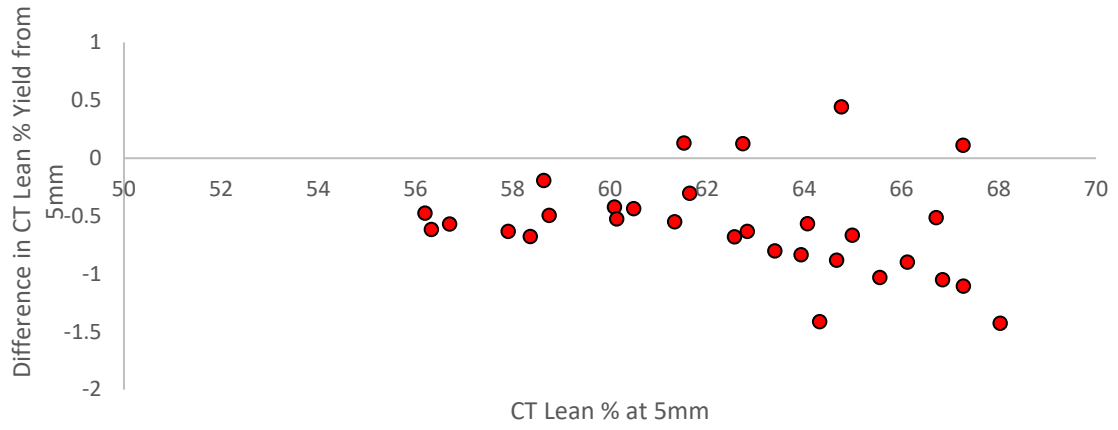
### 3.3. Slice Width

There was little difference in the estimated carcass composition when CT scanning was undertaken at 1mm versus 5mm slice widths. Both carcass Fat % (**Figure 4-a**) and carcass Lean % (**Figure 4 -b**) were strongly aligned, with  $R^2$  values for their relationship in excess of 0.98, and slope values close to 1. The carcass Bone % values were also strongly aligned, although slightly less so, with  $R^2$  values for their relationship greater than 0.96, and slope values close to 1 (**Figure 2-c**). General Linear modelling found no significant difference for the tissue types of Lean and Bone, but a small bias noted for Fat.

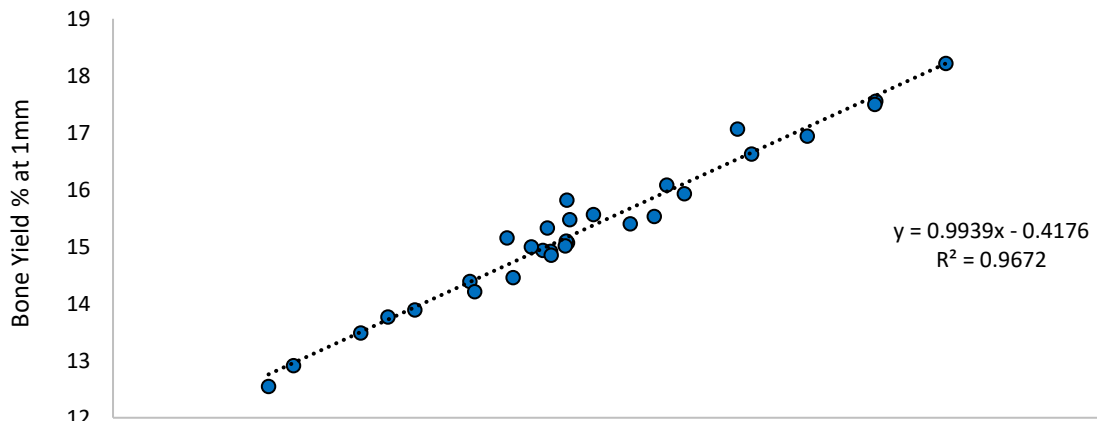




d)



e)



f)

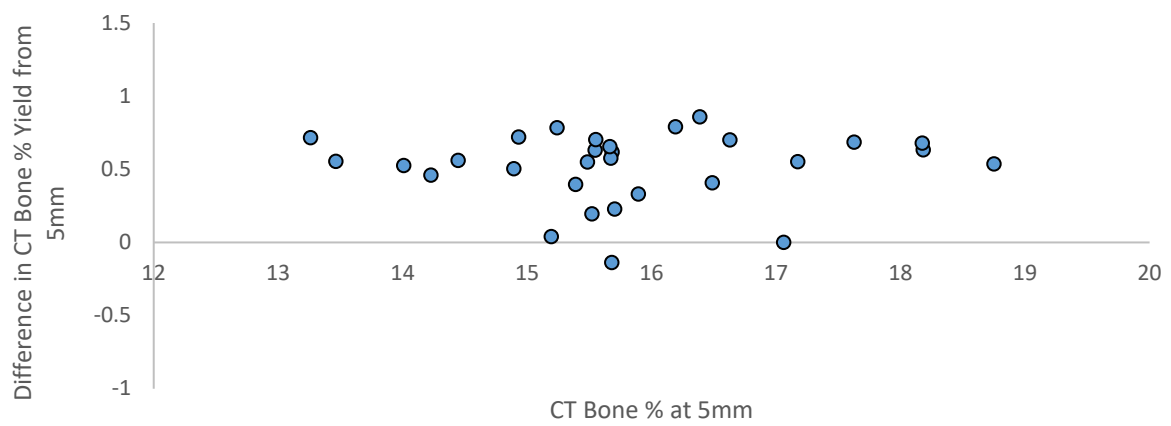


**Figure 12.** A comparison of the CT yield percentages for Fat, **a)** Lean **c)** and Bone **e)** at 5mm slice width vs 1mm slice width across all 20 lamb carcasses and the differences from CT yield % in Fat **b)** Lean **d)** and Bone **f)**.

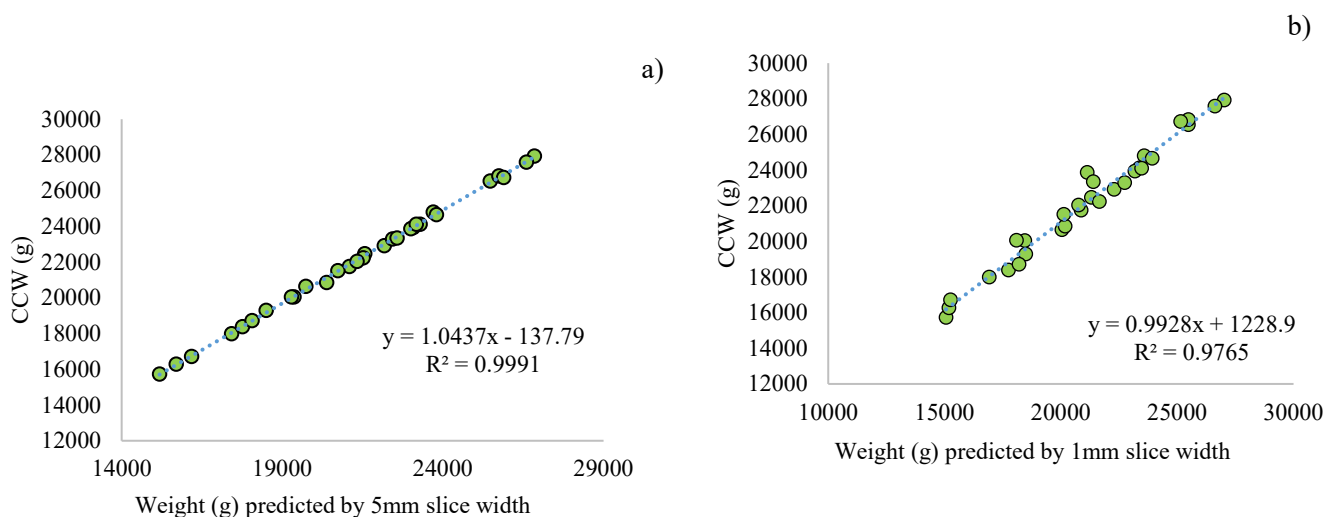


**Figure 13-** Comparison of predicted cold carcass weight (CCW (g)) by CT versus the actual CCW using **a)** 5mm slice width and **b)** 1mm slice width.

### 3.4. Voltage

The equations relating the Hounsfield unit values of bone, lean, and fat voxels scanned at either 100kV or 135kV to the equivalent voxels scanned at 120kV are shown in **Figure 13**. In all cases the fit of these equations was excellent, with  $R^2$  values greater than 0.97. Using these equations, the threshold values at 120kV were transformed into their equivalent values at 100kV or 135kV, as reported in **Table 1**.

**Table 1** – Thresholding Parameters used during image analysis of experiment 1 on voltages 100kV and 135kV.

Voltage	Tissue Type	Threshold limit applied
100kV	Bone	>184
	Lean	2.5 to 184
	Fat	-250 to 2.5
120kV	Bone	>165
	Lean	2.5 to 165
	Fat	-250 to 2.5
135kV	Bone	<157
	Lean	2.5 to 157

	Fat	-250 to 2.5
--	-----	-------------

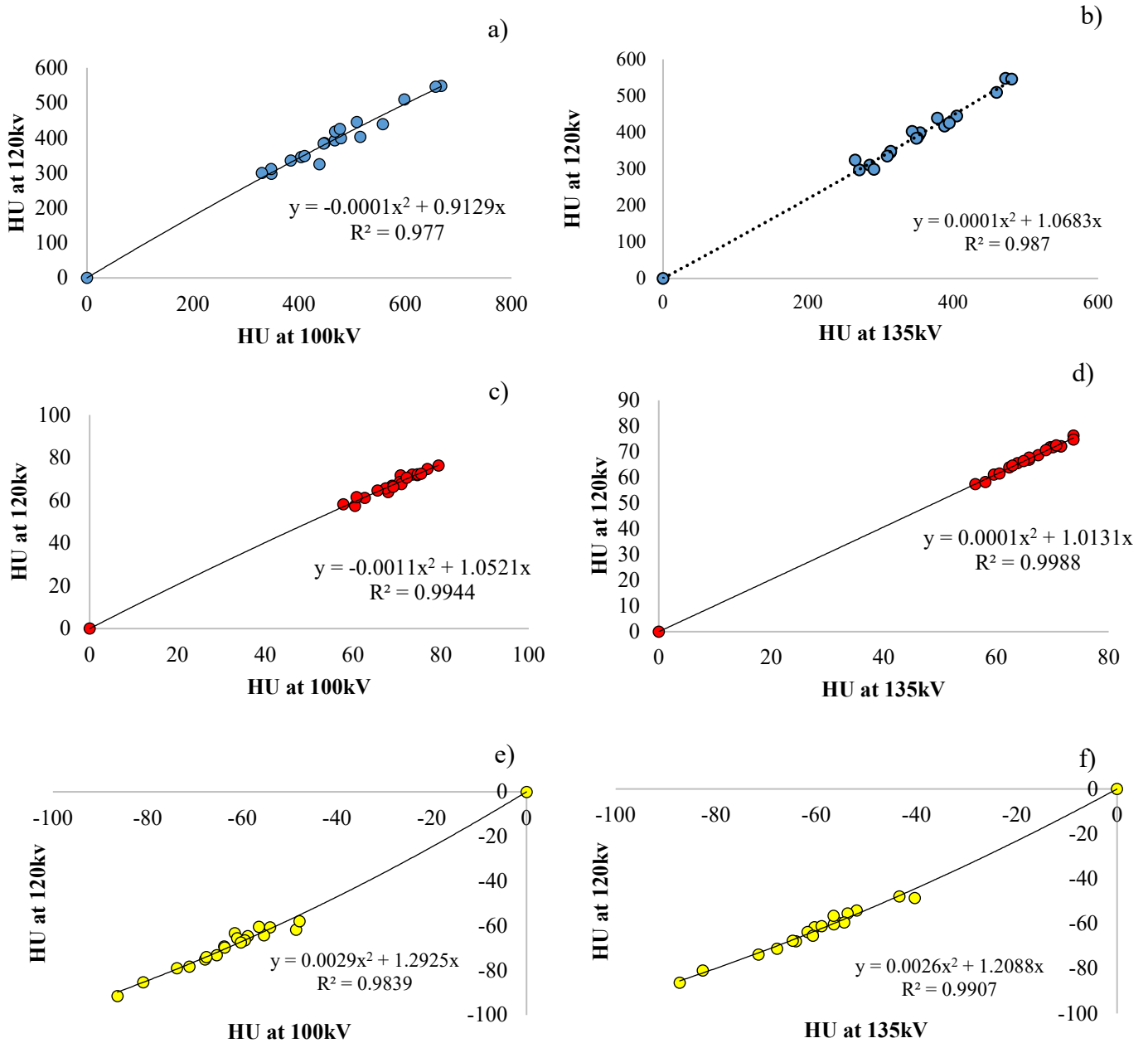


**Figure 14-** Voltage comparisons **a)** Bone at 100kV vs 120kV, **b)** Bone at 135kV vs 120kV, **c)** Lean at 100kV vs 120kV, **d)** Lean at 135kV vs 120kV, **e)** Fat at 100kV vs 120kV, **f)** Fat at 135kV vs 120kV.

### 3.5 Thresholding Adjustments

New threshold parameters were applied along with a new set density for each tissue type and the images reanalyzed. (See methodology on page **Error! Bookmark not defined.**)

Bone showed the largest correction of values post threshold adjustment from the Yield % from the 100kV and 135kV scans to align with the Yield % from the 120kV scans (**Figure 14 e)** and f) Lean yield of muscle also showed better alignment with the Lean Yield predictions at 120kV post adjustment. (**Figure 14, c)** and d)

Fat shows the least change to values before and after threshold adjustment but its 100kV and 135kV yield predictions are also the most closely aligned with the 120kV predictions prior to threshold adjustment. (**Figure 14, a)** and b)

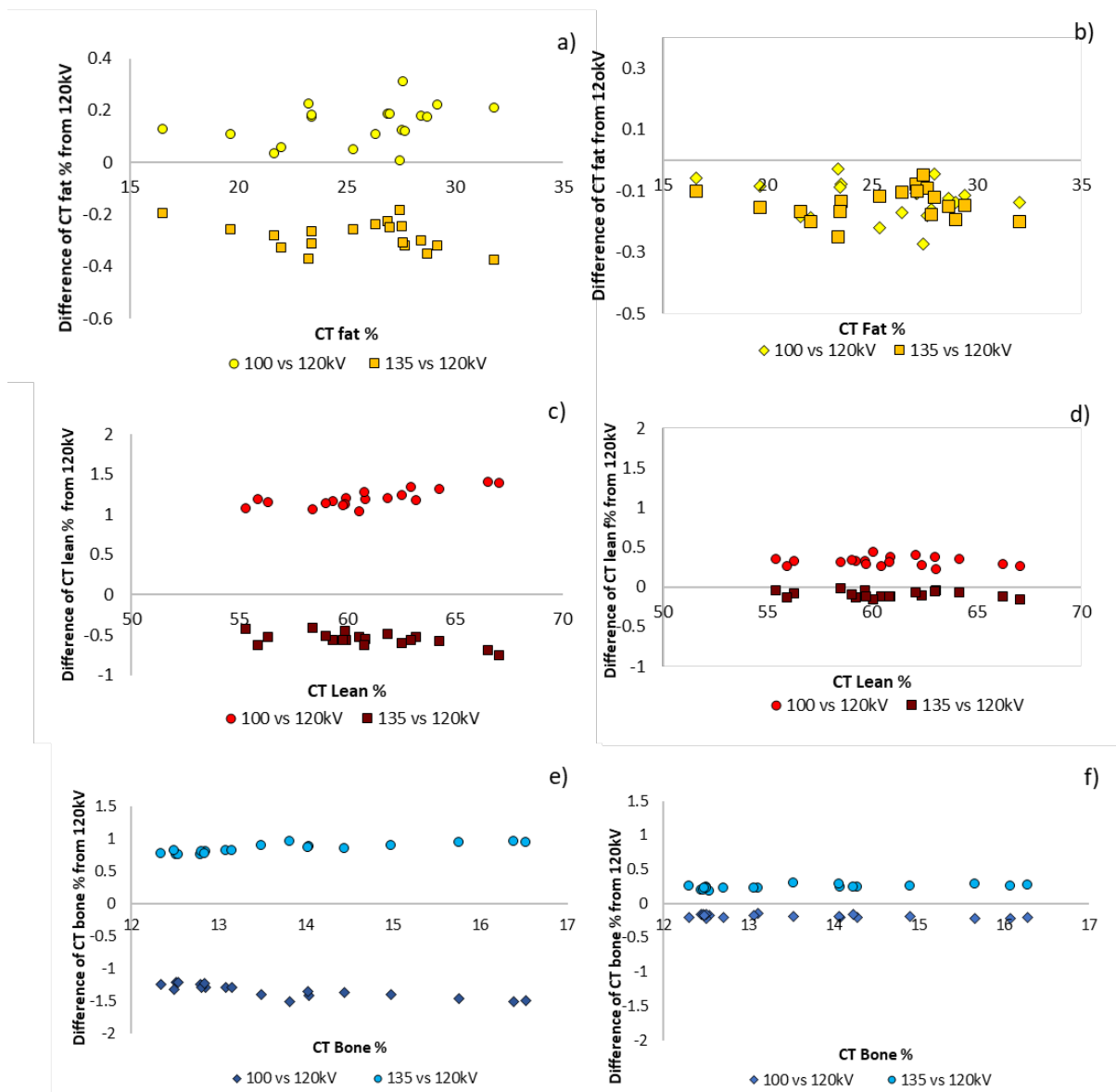


**Figure 15**-Effect of thresholding adjustment on tissue type fat before a) Fat after b) Lean before c) lean after d) Bone before e) Bone after f)

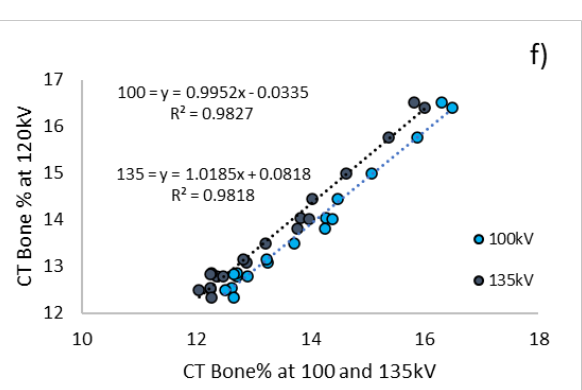
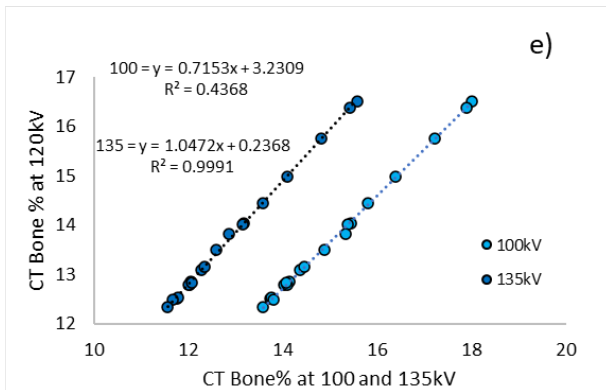
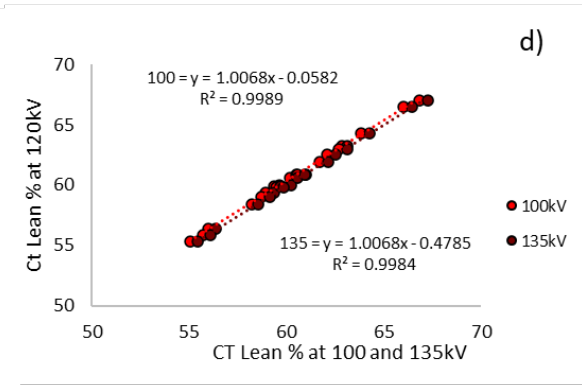
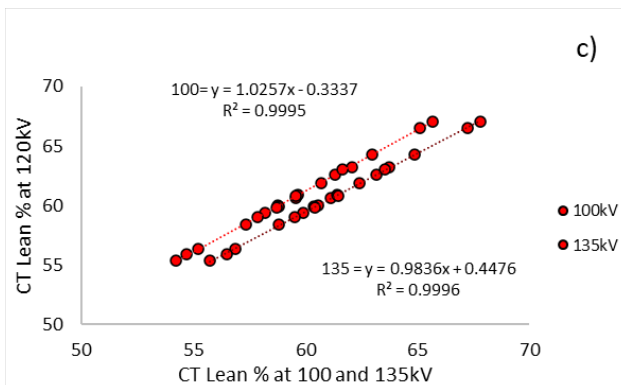
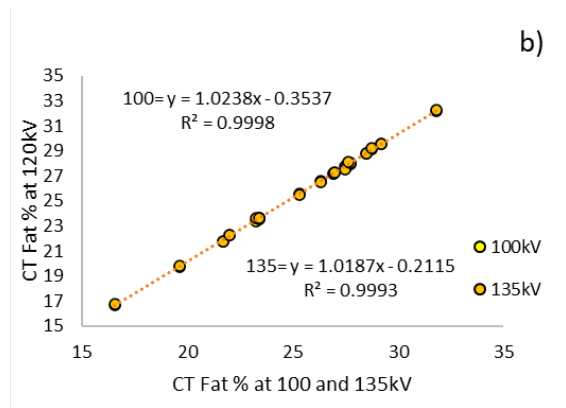
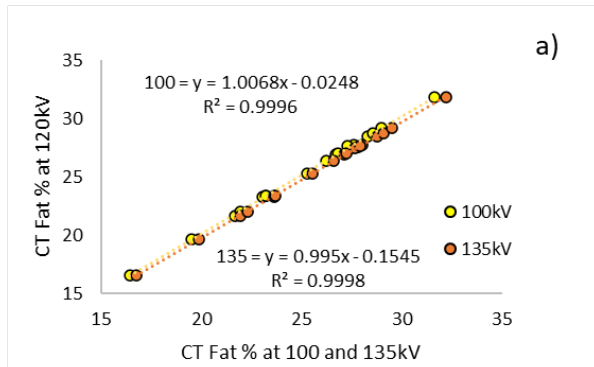


**Figure 16-** CT Yield % at 100 and 135kV compared CT Yield % at 120kV, fat before threshold adjustment a) fat after threshold adjustment b) lean before adjustment c) lean after adjustment d) bone before adjustment e) and bone after adjustment f).

### 3.2.1 Chemical composition

There was a strong association between Chemical protein % and CT Lean % across all carcass sections. The  $R^2$  and RMSE values for the fore, saddle, and hind sections were 0.86 and 2.82% (**Figure 16a**), 0.92 and 2.82% (**Figure 16b**), and 0.91 and 2.20% (**Figure 16c**).

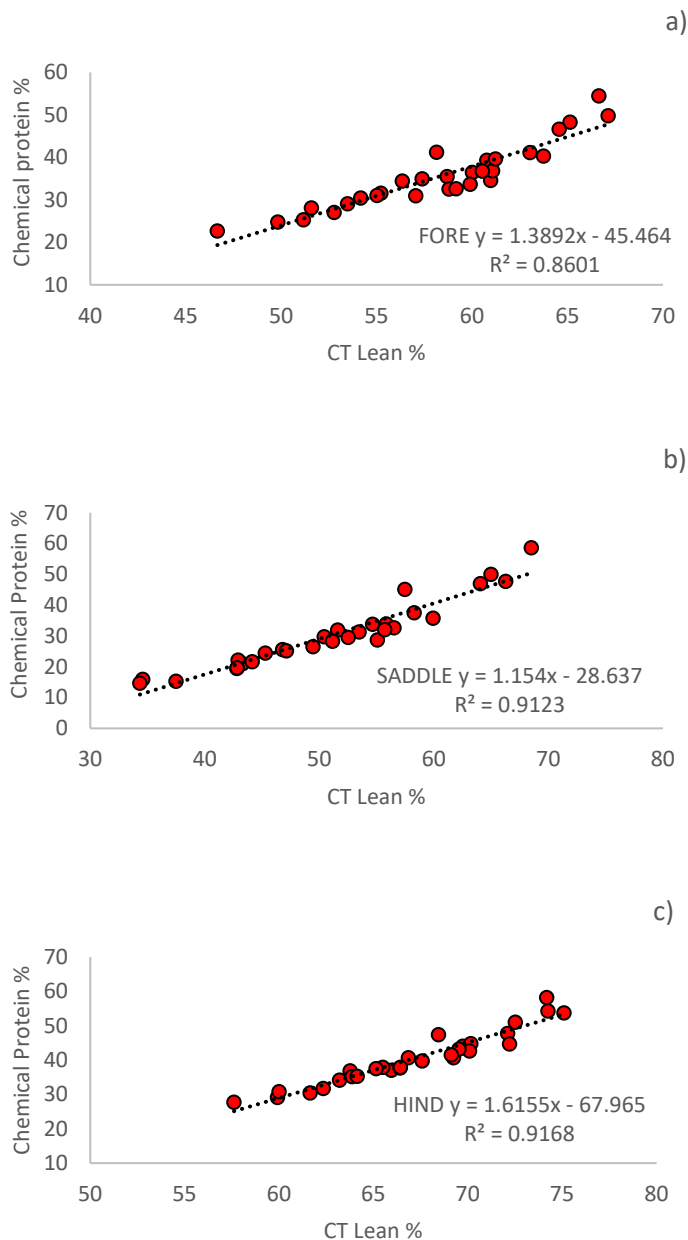


**Figure 16-** CT Lean % vs Chemical protein % in lamb for the a) fore, b) saddle, and c) hind sections of each carcass. Chemical protein values represent the mean of 5 sub-samples.



There was a strong association between Chemical Lipid % and CT Lean % across all carcass sections. The  $R^2$  and RMSE values for the fore, saddle, and hind sections were 0.93 and 2.11% (**Figure 17a**), 0.93 and 3% (**Figure 17b**), and 0.89 and 2.05% (**Figure 17c**).

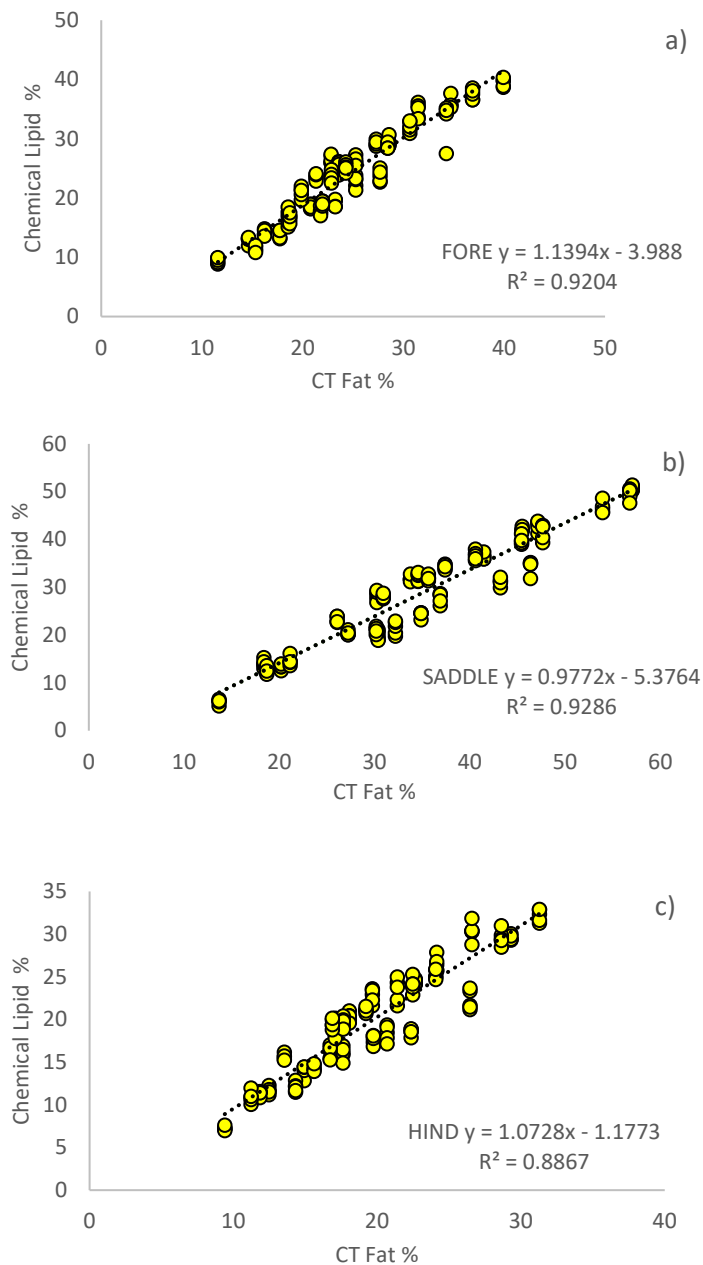


**Figure 17-** CT Fat % vs Chemical Lipid % in lamb for the a) fore, b) saddle, and c) hind sections of each carcass. Chemical lipid % values represent the mean of 5 sub-samples.

### 3.2.1.1 Sampling variability

The variation in values across the 5 sub-samples taken within each lamb carcass section were about 50% higher for Chemical Protein% compared to Chemical Lipid%. This is best represented by the higher coefficient of variation for Chemical Protein %, which is calculated as the standard deviation divided by the mean of the values. The minimum and maximum range of these values was also greater for Chemical Protein %, with a range of 16.1% (**Table 2**), compared to Chemical Lipid % variability with a range of 7.7 % (**Table 2**).

*Table 2-Minimum, Maximum, Standard Deviation and Coefficient of Variation for the variation between the 5 sub-samples taken within each carcass section to determine Chemical Protein % and Chemical Lipid% in lamb. These variation values were calculated within each set of 5 sub-samples, by subtracting the mean of the 5 sub-samples from the individual sample value.*

	<b>Chemical Protein %</b>	<b>Chemical Lipid %</b>
<b>Minimum</b>	-5.04	-5.701
<b>Maximum</b>	11.06	1.995
<b>Standard Deviation</b>	1.583	0.767
<b>Coefficient of variation</b>	0.045	0.032

## 3.3 Discussion

### 3.3.1 Immediate Repeatability

As expected, the CT estimated Bone%, Lean% and Fat% demonstrated excellent repeatability across 3 consecutive scans taken at the same voltage (120kV). The  $R^2$  for the relationship between these scans was so close 1 (0.9999), and the maximal difference between them was so small (0.05 of a percentage unit for fat and lean), that these values could be considered highly repeatable. This result demonstrated the robustness of this methodology as a gold-standard measurement for calibrating other technologies. By contrast, the repeatability of other methods for determining composition, including manual dissection and grinding carcasses to demonstrate chemical composition, are destructive and therefore repeatability cannot be demonstrated. Hence the high repeatability provided industry with confidence of this method as a calibrating standard.

### 3.3.2 Cut vs Whole

Contrary to our expectations, sectioning carcasses prior to CT scanning caused a reduction in estimated Lean% and an increase in estimated Fat%, although only a small reduction in estimate bone%. These effects can be explained by the increase in surface to volume ratio resulting in more partial averaging of near-surface voxels with air. For those voxels affected, this would reduce their voxel values, resulting in those closer to the surface being more likely to partition into the lower density tissue types – hence the increase in fat and reduction in lean. The comparatively smaller change in bone percentage is reflective of the smaller portion of bone in the carcass, hence the change in bone is proportionately similar to the changes seen for lean and fat tissue.

While these changes in tissue proportions were measurable, they were also highly consistent across carcasses. For this reason, the  $R^2$  values for the relationship between cut versus whole carcass scans were greater than 0.99 for each of the bone%, muscle% and fat%. This meant that carcass sectioning was not likely to cause re-ranking between carcasses that vary in the composition. None-the-less, the changes in estimated composition need to be accounted for when comparing datasets where sectioning has been imposed.

Over the last decade carcass sectioning of lambs has been an essential component of the nucleus flock CT scanning protocol, as it simplifies the analysis of tissue distribution between fore, saddle, and hind sections. To maintain consistency with this approach, and the capacity to determine regional tissue distribution, the carcass sectioning will remain the standardized method. However, given the magnitude of this effect the sectioning process needs to be carefully specified and adhered to during scanning to act as part of the calibration protocol for other devices.



### **3.3.3 Slice Width**

Slice width was found to influence tissue yield predictions, with CT estimates for 1mm slice widths slightly higher for lean% and slightly less% for bone, although unchanged for fat%. While this highlights the need for standardization of this protocol, it is not immediately clear which slice width delivers the best results. Future data will test the alignment with chemical composition, however in this study we were able to compare the sum of all components with estimates of carcase weight. In this case the 5mm slice width showed the strongest association, suggesting that it has the most precision for estimating volume. This also aligns with our standardized protocol for scanning nucleus flock lambs, as well as the European position on CT where they have adopted 5mm as the standard slice width for assessing pork composition. Therefore, at this point 5mm slice width will be retained as the optimal width for determining carcase composition in lamb carcasses.

### **3.3.4 Voltage**

As indicated by the results, increasing voltage decreases the Hounsfield unit value for both bone and lean, while the opposite occurred for fat. Bone was the most affected with the Hounsfield unit values at 100kV and 135kV differing by about 150 HU, while the other tissues were less affected with Lean varying by less than 3 HU and Fat less than 5HU.

This differential variation in Hounsfield unit value for each tissue type implied that the current method of allocating pixels into Fat, Lean or Bone based on fixed HU thresholds caused re-allocation of pixels as voltage changes, mainly between bone and lean, causing the overall composition percentages for each tissue type to shift. By amending these thresholds to match the voltage used, we attempted to correct for this error. After reprocessing the images using these adjusted thresholds the estimated carcase composition was found to be more consistent across voltages, although small discrepancies still exist. Future analysis will attempt to correct for this error by referencing components within a commercially available synthetic phantom (XTE CT phantom).

The long-term result will be that no matter what a machine's make and model and its voltage capabilities, by applying a set algorithm we can realign all composition values to those of 120kV, standardizing the CT carcase predictions. However, when using CT to calibrate other technologies to predict carcase composition, this should always be captured at a set voltage of 120kV with the inclusion of phantom scans to correct for machine differences.

### **3.3.5 Chemical composition of lamb**

As expected, CT Lean % predictions demonstrated a good association with Chemical Protein %, but there was some variation to this relationship seen between sections. A higher  $R^2$  was noted for the saddle and hind sections ( $R^2$  0.92 and  $R^2$  0.91 respectively) vs  $R^2$  0.89 for the fore. Similarly, CT Fat % predictions showed a strong association with Chemical lipid %, in this case with only minor variations between sections. These strong associations demonstrate that CT Lean % and CT Fat % can predict chemical protein and fat composition in lamb, demonstrating its equivalence to this historical measure of carcass composition.

Chemical analysis for both protein and lipid showed marked sub-sample variation. Despite 6 course mixings during grinding, two plate sizes, and considerable fine-grind mixing post freeze drying, residuals of up to 11 protein percentage units from the mean and 6 fat percentage units from the mean were still present between subsamples. This variation can be compared to the repeatability results for CT using the “within sub-sample” coefficient of variation value. For Chemical Protein% and Fat% these values were 0.045 and 0.032 for lamb. By contrast, the coefficient of variation values for the repeatability of CT Lean% and CT Fat% were 0.00027 and 0.00072 for lamb – several orders of magnitude smaller. This variation in sampling makes calibration of objective measurement tools against chemical analysis an unreliable method when compared to CT. Furthermore, CT has the advantage of being non-destructive.

### 3.4 Conclusions

These experiments demonstrated the capacity of CT to deliver highly repeatable, non-destructive estimates of carcass composition. This is an essential attribute for CT to act as a calibrating gold standard against which other lean meat yield measurement technologies can be accredited. We also explored a range of factors that can impact these estimates, demonstrating the need to carefully standardize these at the point of scanning. This includes carcass sectioning, CT slice width, and CT voltage at the point of scanning. While adjustments can be made to account for these effects, standardizing the scanning protocol will eliminate this requirement. To ensure the best estimate of carcass composition, and to be consistent with previous studies this standardized protocol should include scanning at 120kV, CT image slice widths of 5mm, and sectioning the carcass into fore, saddle and hind sections.

## 4. The repeatability of CT scanning in Beef

### 4.1 Methodology

#### 4.1.1 Experiment 1- bone-in short loin and rib sets

Experiment 1 assessed the impact of freezing and thawing on beef bone-in shortloins and ribsets from 15 animals and the CT prediction of carcass Lean%, Bone% and Fat%. It also assessed the impact of slice width on the CT carcass composition prediction.

##### 4.1.1.1 Carcass Selection

15 carcasses were selected from the Teys, Wagga Wagga abattoir. Carcasses were selected to maximise the phenotypic range in P8 fat depth with a mean $\pm$ STDEV of 13.4mm ( $\pm$ 7.2) and hot standard carcass weight (HSCW) with a mean $\pm$ STDEV of 315.6kg ( $\pm$ 74.22). From each carcass a bone-in shortloin and a rib-set was dissected and transported to Murdoch University for CT scanning 15 days post slaughter.

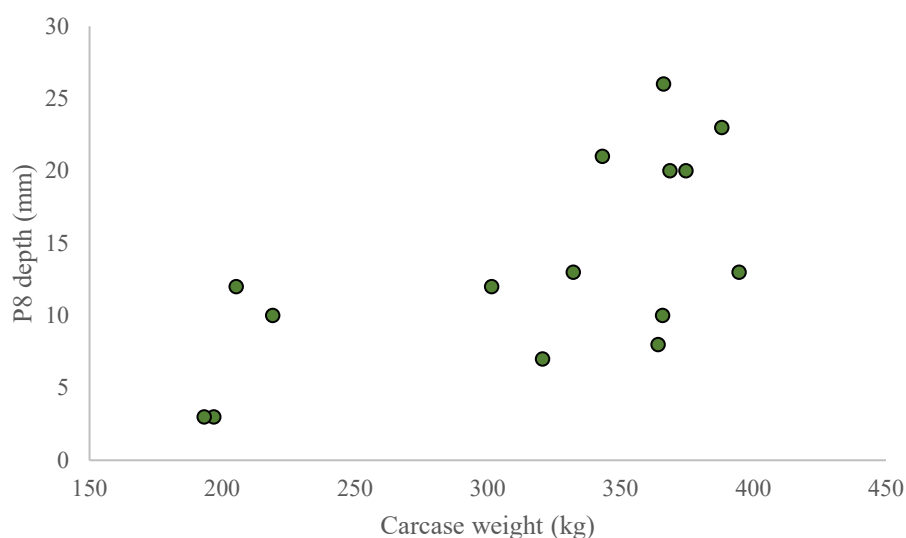


**Figure 18.** Carcass weight (kg) vs P8 fat depth (mm) for carcasses selected in Experiment 1.

##### 4.1.1.2 CT scanning

Carcass sections were CT scanned using a Canon Aquilon Lightning scanner with Pilot scan length 1500mm, Dynamic mAs with set min/max parameter of 50 to 300mAs, FOV 500mm, rotation 0.75secs, Pitch factor 0.813, Helical pitch 65, Voltage 135kV. Images were captured at a 1mm slice width and also reconstructed into 5mm slice widths. After the initial scanning, carcass sections were frozen and then scanned, and then thawed and scanned for a third time.

#### 4.1.1.3 Image analysis

For all scans captured at 135kV, the Raw DICOM images were analysed using ImageJ software (version 1.52a, National Institutes of Health, Bethesda, MD, USA in combination with Microsoft excel). Within images non-carcass portions of the image were removed, and the remaining voxels were categorized into bone, lean and fat. The allocation of pixels to tissue type was based on fixed thresholds where fat was defined as voxels at -250 to 2.5HU, lean at 2.6-165HU and bone at >165HU. Volume estimation was calculated using the Cavalieri stereological method illustrated in the following equation. (Gundersen, Bendtsen, Korbo, Marcussen, & Møller, 1988; Gundersen & Jensen, 1987)

$$\text{Volume}_{\text{Cav}} = d \times \sum_{g=1}^m \text{area}_g - t \times \text{area}_{\text{max}}$$

Where  $m$  represents the quantity of CT scans taken,  $d$  is the slice width (10mm),  $t$  representing the thickness of the slice (slice width) which in this experiment was 10mm.  $\text{area}_{\text{max}}$  represents the maximum area of all scans taken.

Mass was then calculated for each tissue type by averaging the HU of all pixels within each component, converting to voxel mass based upon a linear density transformation (Mull, 1984), and then multiplying by the number of voxels for that tissue type. This allowed the calculation of the weight (kg) of each tissue type (bone, lean and fat), which was then expressed as a percentage of total carcass weight at the time of CT scanning.

#### 4.1.1.4 Statistical analysis

The effect of slice width was assessed in the first instance using a GLM, where CT fat % estimated from slice widths of 5mm were used as the dependent variable, and CT fat % estimated from slice widths of 1mm were tested as the independent variable. The slope of this relationship, the bias estimated at the mean of the CT fat% values, the RMSE and the  $R^2$  were reported to indicate the alignment of these estimates. Secondly, the difference between the CT fat% values estimated at 1mm and 5 mm were calculated, and then regressed against the CT fat % estimated at 5 mm to test for any significant deviation from zero along this continuum. This analysis was repeated for CT lean% and CT bone%.

The effect of freezing and thawing was assessed in the first instance using a GLM, where CT Fat % estimated from fresh rib and shortloin sections were used as the dependent variable, and CT Fat % estimated from frozen and then thawed sections were tested as the independent variable. The slope of this relationship, the bias estimated at the mean of the CT fat% values, the RMSE and the  $R^2$  were reported to indicate the alignment of these



estimates. Secondly, the difference between the CT Fat% values estimated for frozen and thawed sections from the CT Fat% values estimated for the fresh sections were calculated, and then regressed against the CT Fat % estimated for the fresh sections to test for any significant deviation from zero along this continuum. This analysis was repeated for CT lean% and CT bone%.

#### 4.1.2 Experiment 2- Beef butts and Aitch bone

Experiment 2 determined the impact of voltage on estimates of carcass Bone %, Fat % and Lean% of beef butt sections.

##### 4.1.2.1 Carcass selection

30 carcasses were selected from the Dardanup Butchering company slaughter floor. Carcasses were selected to maximise the phenotypic range in P8 fat depth with a mean $\pm$ STDEV of 11.2mm ( $\pm$ 6.12) mm and hot standard carcass weight (HSCW) with a mean $\pm$ STDEV of 286.7kg ( $\pm$  56.95).

The butt sections were separated from the carcasses and kept chilled at 5°C post slaughter until CT scanning 5 days later.

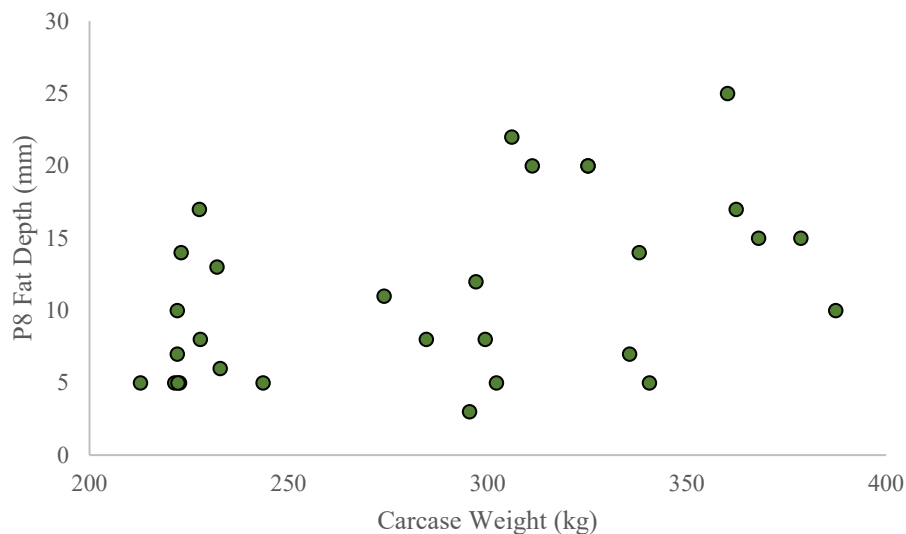


Figure 19. Carcass Selection-Experiment 2- Carcass weight (kg) vs P8 fat depth (mm).

##### 4.1.2.2 CT scanning

The scanning parameters were identical to Experiment 1 except three voltages were used including 100kV, 120kV and 135kV. During consecutive voltage scans the beef butts were not moved until the scanning protocol was complete. Veterinary X-ray tape was wrapped

tightly around the largest butts to enable entrance into the CT spiral through the set FoV of 500mm.

Plastic phantoms with known densities were also scanned at each voltage before, during and after the carcasses.

#### 4.1.2.3 Image analysis

The image analysis of scans captured at 100kV and 135kV was undertaken in two ways. Firstly, the same method described above for the scans captured at 135kV was applied to the 100kV and 120kV scans. Secondly, these scans were re-analysed using a separate set of thresholds to allocate voxels to bone, lean and fat components. To determine these thresholds a single cross-sectional image from each butt section was selected within the 120kV scans. Within this image 3 regions of interest consisting of at least 50 pixels were identified anatomically to consist of bone, lean, and fat tissue, and their average Hounsfield unit value calculated. These same voxels were then matched to those in the corresponding scans taken at 100kV and 135kV, to determine the average Hounsfield unit value for these same pixels at 100kV and 135kV. This process was repeated for each butt section, producing 30 separate estimates of average Hounsfield unit value for bone, lean, and fat tissue at voltages of 100kV, 120kV, and 135kV, a total of 270 separate values. A conversion equation was then established enabling the transformation of HU values from those scanned at 120kV into their 100 or 135kV equivalent values. For the bone average Hounsfield unit value, firstly estimates taken at 100kV were regressed against those taken at 120kV, and then secondly estimates taken at 135kV were regressed against those taken at 120kV. This process was repeated for the fat and lean values, establishing transformation equations (see **Figure 30**, **Figure 31**, **Figure 32**) which were then applied to the threshold values set at 120kV enabling conversion of the thresholds into their 100 or 135kV equivalent values which are shown in **Table 3**. These new threshold values were then applied to the scans captured at 100kV and 135kV, using the same image analysis method described in section 3.1.3 above. The only difference was that rather than applying the Mull linear transformation (Mull, 1984) to convert to density(kg/L) and mass estimation, fixed values of tissue density were applied instead. The voxels allocated as bone were multiplied by a fixed density of 1.43g/cm<sup>3</sup>, lean by 1.078g/cm<sup>3</sup>, and fat by 0.94 g/cm<sup>3</sup>. The Image analysis protocol for Experiment 1 was repeated but also included 100kV and 120kV scans.

#### 4.1.2.4 Statistical analysis

To analyse the effect of voltage on CT scan estimates of composition, the CT estimates of Fat% at 120kV were regressed against the CT Fat% estimates from scans at 100kV and 135kV. This was done twice, firstly for the estimates prior to applying the threshold adjustment, and then after applying the threshold adjustment. In addition, the difference in CT Fat% estimates from scans at 100kV and 135kV minus those taken at 120kV was calculated and then this was

regressed against the CT Fat% at 120kV. This process was repeated for CT Lean% estimates and CT Bone% estimates.

#### **4.1.3 Beef Chemical composition**

##### **4.1.3.1 Carcase selection**

30 Beef butts were selected from the Dardanup Butchering Company slaughter floor during routine processing at the DBC abattoir in Dardanup, WA across two separate weeks in March and April 2021. As shown in Figure 19 above, a wide phenotypic range was selected with Hot Standard Carcase Weights (HSCW) varying from 212kg to 387kg and P8 fat depth varying from 3mm fat to 25mm fat.

##### **4.1.3.2 CT scanning**

The whole carcasses were sectioned into Butts containing the Aitch bone and this cut was transported by refrigerated logistics to Murdoch University in 2 batches of 15 animals one week apart where they were weighed on arrival and kept in refrigerated storage before scanning within 24hrs.

Carcasses were CT scanned using a Canon Aquilon Lightning machine with Pilot scan length 1500mm, Dynamic mAs with set min/max parameter of 50 to 300mAs, FOV 500mm, rotation 0.75secs, Pitch factor 0.813, Helical pitch 65, Voltages 100kV, 120kV and 135kV. Images were captured at a 1mm slice width and also reconstructed into 5mm slice widths.

Phantoms of known density including the XTE-CT Phantom, were scanned before, during and after the 30 beef butts to assess for any drift in Hounsfield units over the day.

##### **4.1.3.3 Image analysis**

Image analysis was undertaken using the same protocols as described in section 3.1.1.3 above, using the thresholds specified for all three voltages as listed in **Table 3**.

##### **4.1.3.4 Chemical composition sampling**

Once CT scanning was completed the carcasses were de-boned by an experienced butcher/boner who removed all visible soft tissue including tendons at their attachment sites, soft cartilage was also included in the soft tissue grind up. Once the bone was

removed, the leg bone and patella were weighed and recorded followed by the Aitch bone. The remaining soft tissue was weighed and then ground into mince.

The soft tissue was first passed twice through a large mincing plate with holes of 30mm diameter, then again twice through a plate with 5mm holes a uniform and homogenous mix was created, this was then manually mixed again prior to sampling. Any larger tendon sections which were unable to be processed by the mincer due to their density were weighed and kept separate for analysis later to and their results will be added back in to total soft tissue calculation.

5 sub samples of approximately 50g wet weight each were taken into plastic lidded tubes for each animal (total 250g per animal).

#### **4.1.3.5 Chemical composition analysis**

The same protocol was used for chemical analysis as outlined in lamb section 3.1.3.4.

#### **4.1.3.6 Statistical analysis**

The same Statistical analysis protocol was used as outlined in lamb section 3.1.3.5 with the removed step of the lamb NIR equation and addition of SNV mathematical conversion as the absence of bone rendered it useless.

## 4.2 Results

### 4.2.1 Slice Width

There was little difference in the estimated butt composition when CT scanning was undertaken at 1mm versus 5mm slice widths. Butt Fat% (**Figure 20a**), Lean % (21c), and Bone % (**Figure 22e**) were all strongly aligned, with  $R^2$  values for their relationship in excess of 0.99, and slope values close to 1. There were small differences in the estimated composition values for the tissue types of Fat% and Bone%, and in all cases these changed with changing composition. CT Fat% estimated at 5mm was as much as 0.5% units less in butts with higher CT Fat% values ( $p < 0.001$ ,

**Figure 22b**). For CT Lean% this was as much as 0.2% units less in higher CT Lean% butts ( $p < 0.001$ , **Figure 21d**), and for CT Bone% it was as much as 0.35% units more in higher CT Lean% butts ( $p < 0.001$ ,

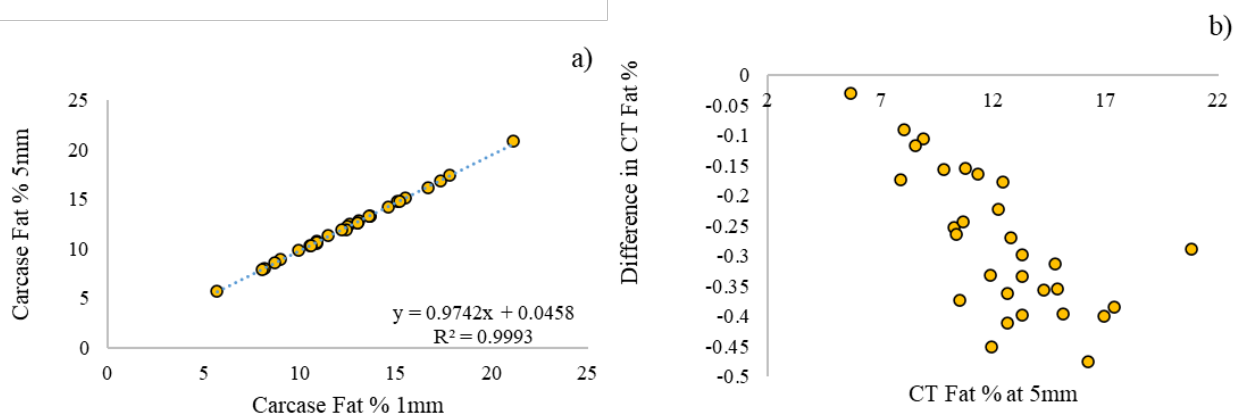


**Figure 20.** Comparison of a) the CT Fat% estimated using 5mm slice width versus 1mm slice width, and b) the difference in estimated CT Fat% between slice widths, represented as 5mm minus 1mm.

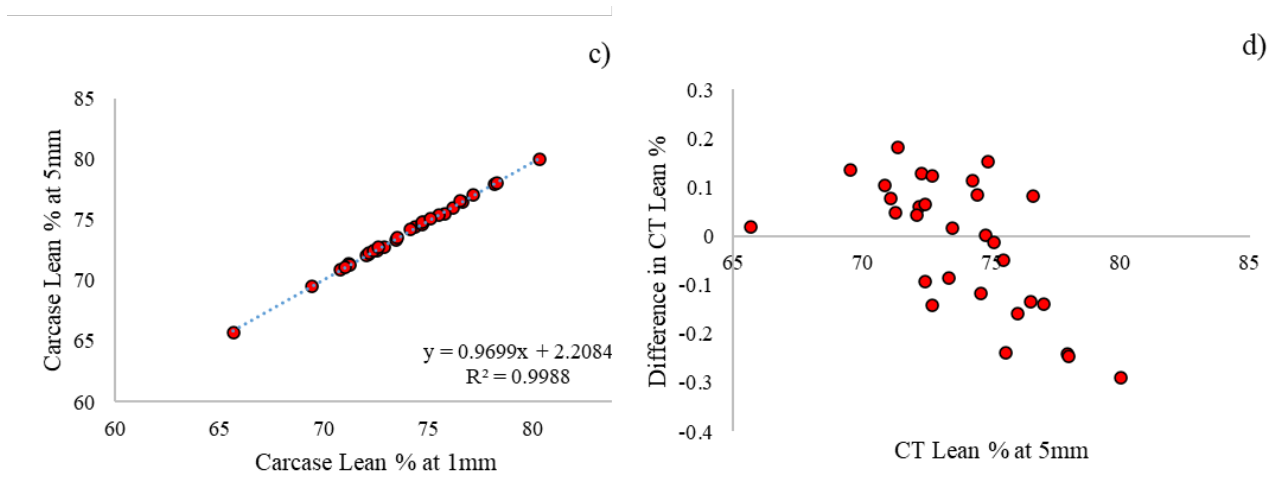


**Figure 21.** Comparison of c) the CT Lean% estimated using 5mm slice width versus 1mm slice width, and d) the difference in estimated CT Lean% between slice widths, represented as 5mm minus 1mm

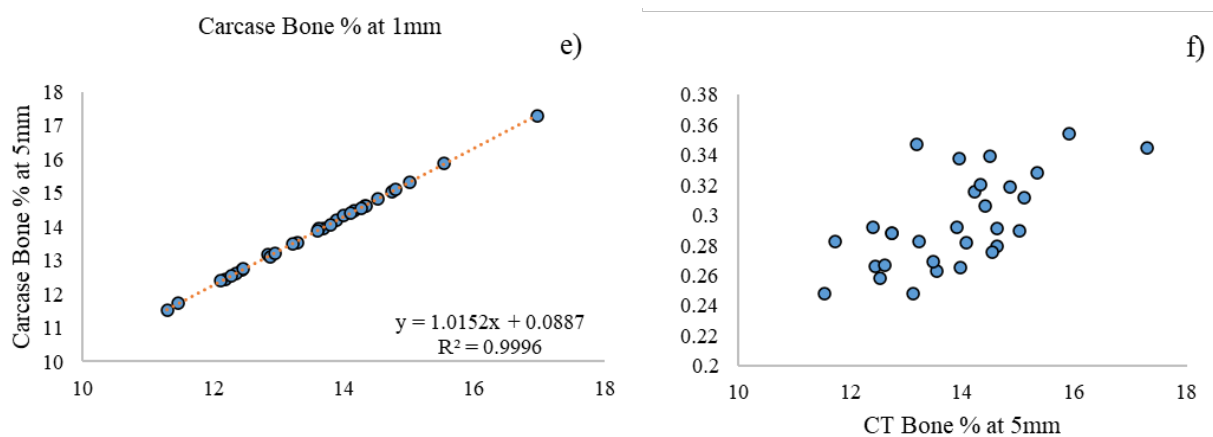


**Figure 22.** Comparison of e) the CT Bone% estimated using 5mm slice width versus 1mm slice width, and f) the difference in estimated CT Bone% between slice widths, represented as 5mm minus 1mm.

With respect to estimating butt weights, both the 1 and 5mm slice widths slightly over-estimated butt weights, although the 1mm error was slightly greater with over-estimates of 200-300g, double that of the 5mm slice width (**Figure 23**).

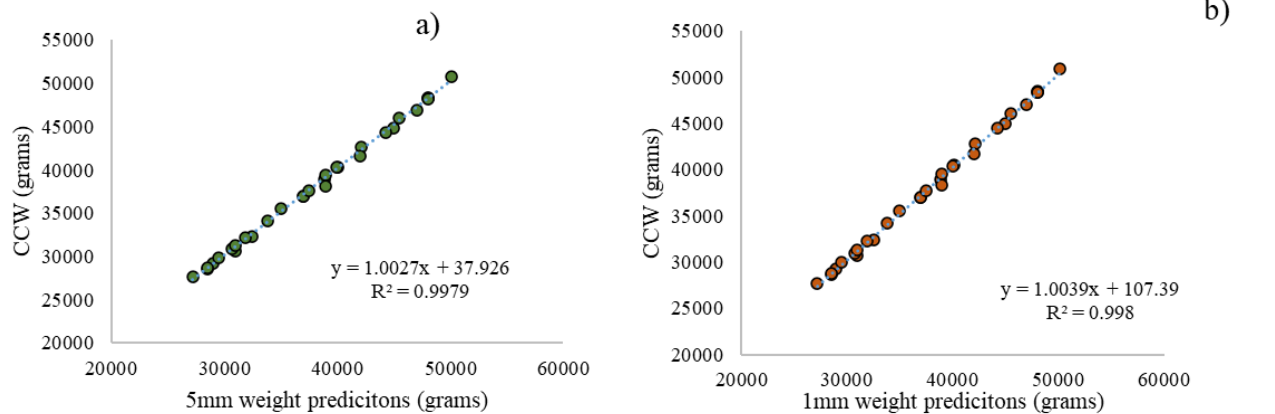


**Figure 23.** Comparison of predicted cold carcass weight (CCW (g)) by CT versus the actual CCW using a) 5mm slice width and b) 1mm slice width.

## 4.2.2 Freeze/Thaw comparison

### 4.2.2.1 Rib sets

There was a considerable difference in composition estimates for Frozen vs Thawed rib-sets when compared to Fresh rib-sets. The thawed composition predictions were closely aligned with the fresh with the  $R^2$  for all three tissue types above 0.98 (**Figure 24a**, **Figure 25a**, **Figure 26a**). The frozen predictions showed poor precision for both Fat% and Lean% with an  $R^2$  of less than 0.25 (**Figure 24a**, **Figure 25a**). In contrast Bone% maintained its strong association with Fresh composition ( $R^2$  of 0.99), irrespective of whether it was thawed or frozen (**Figure 26a**). The differences graphs show that the thawed Fat%, Lean% and Bone% CT predictions varied little from Fresh CT predictions, with Fat% having an average difference of  $-0.47 \pm 0.318\%$  (**Figure 24b**), Lean an average difference of  $0.56 \pm 0.378\%$  (**Figure 25b**) and Bone an average difference of  $-0.08 \pm 0.197\%$  (**Figure 26b**). In contrast, Frozen results were vastly different for both Fat% and Lean% with an average difference of  $-34.39 \pm 3.575\%$  for Fat% (**Figure 24b**) and  $33.86 \pm 3.589\%$  for Lean% (**Figure 25b**), although little difference for frozen bone % with an average difference of  $0.52 \pm 0.137\%$  (**Figure 26b**).

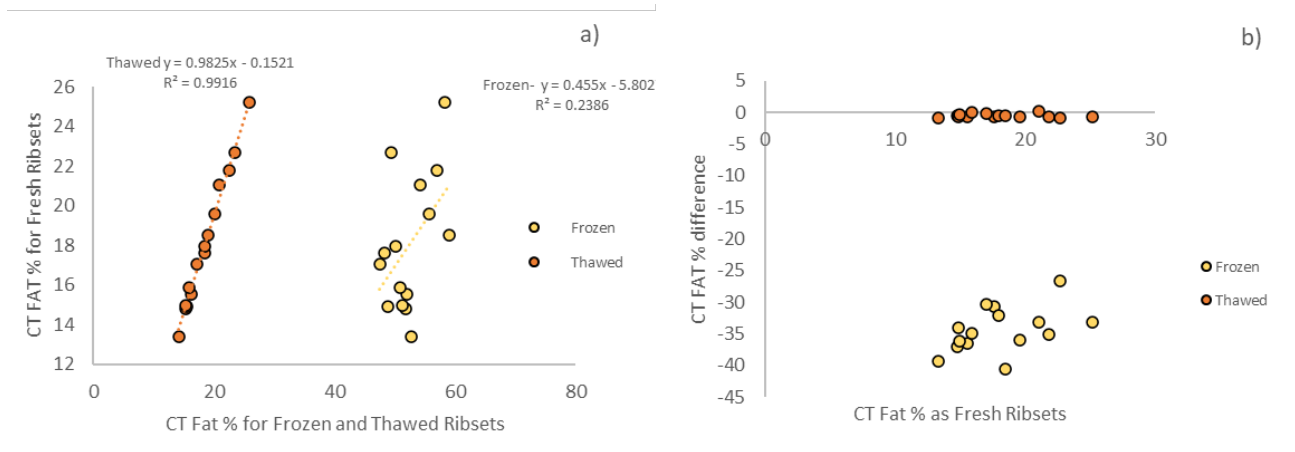


**Figure 24-** Comparison of a) CT Fat % predictions for fresh rib-sets versus frozen and thawed rib-sets, and b) CT Fat% differences for fresh rib-set values minus frozen or thawed rib- set values versus CT Fat% for fresh rib-sets.

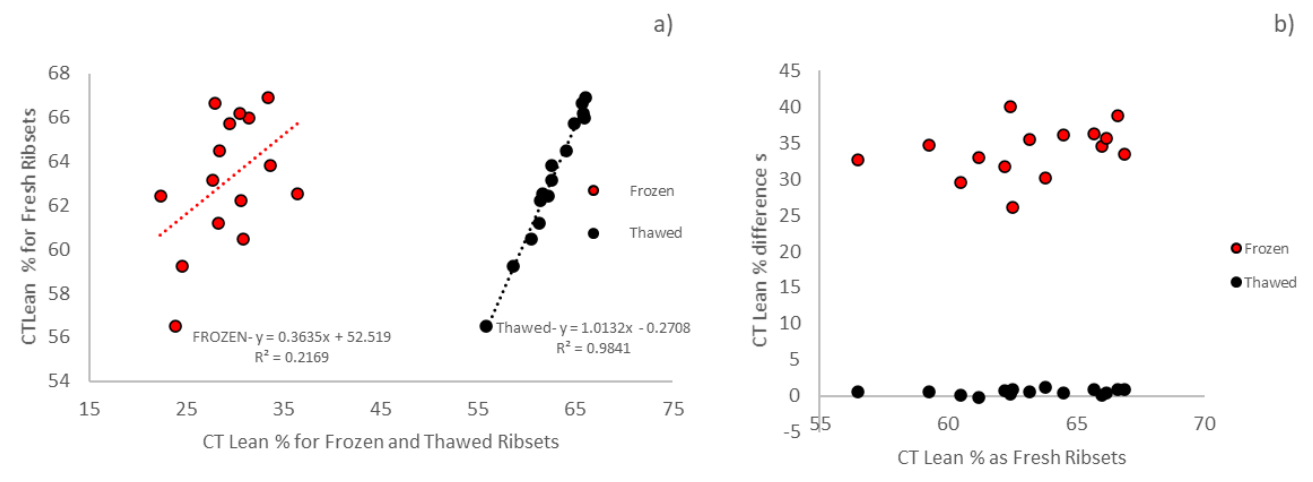


**Figure 25-** Comparison of a) CT Lean% predictions for fresh rib-sets versus frozen and thawed rib-sets, and b) CT Lean% differences for fresh rib-set values minus frozen or thawed rib- set values versus CT Lean% for fresh rib-sets.



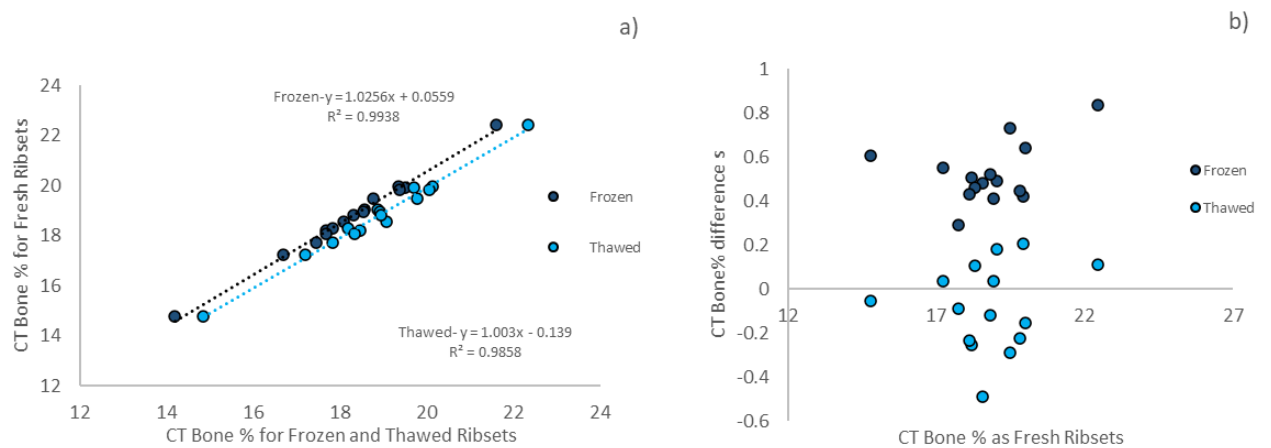


**Figure 26-** Comparison of **a)** CT Bone% predictions for fresh rib-sets versus frozen and thawed rib-sets, and **b)** CT Bone% differences for fresh rib-set values minus frozen or thawed rib-set values versus CT Bone% for fresh rib-sets.

#### 4.2.2.2 Short loin

Similar results were seen with the bone-in short-loin where again the thawed prediction for fat% (**Figure 27a**), lean% (**Figure 28a**) and bone% (**Figure 29a**) all showing a strong association with fresh short-loins, with  $R^2$  above 0.99. Frozen again showed poor precision for both fat% and lean% with an  $R^2$  of  $< 0.59$ . Bone was not affected by freezing, with both frozen and thawed short-loins demonstrating a strong association with the fresh CT prediction with an  $R^2$  of 0.999.

The differences graphs again showed that the fat% (**Figure 27b**), lean% (**Figure 28b**) and bone% (**Figure 29b**) predictions of the thawed cuts had minimal differences from fresh with average differences of  $-0.28 \pm 0.239\%$ ,  $0.45 \pm 0.216\%$  and  $-0.17 \pm 0.131\%$ . Frozen again showing large differences for fat% (**Figure 27b**) and lean% (**Figure 28b**) with average differences of  $-19.21 \pm 3.259\%$  and  $18.70 \pm 3.23\%$ . Bone was again closely aligned with the fresh CT bone% prediction with an average difference of only  $0.52 \pm 0.115\%$  (**Figure 29b**).

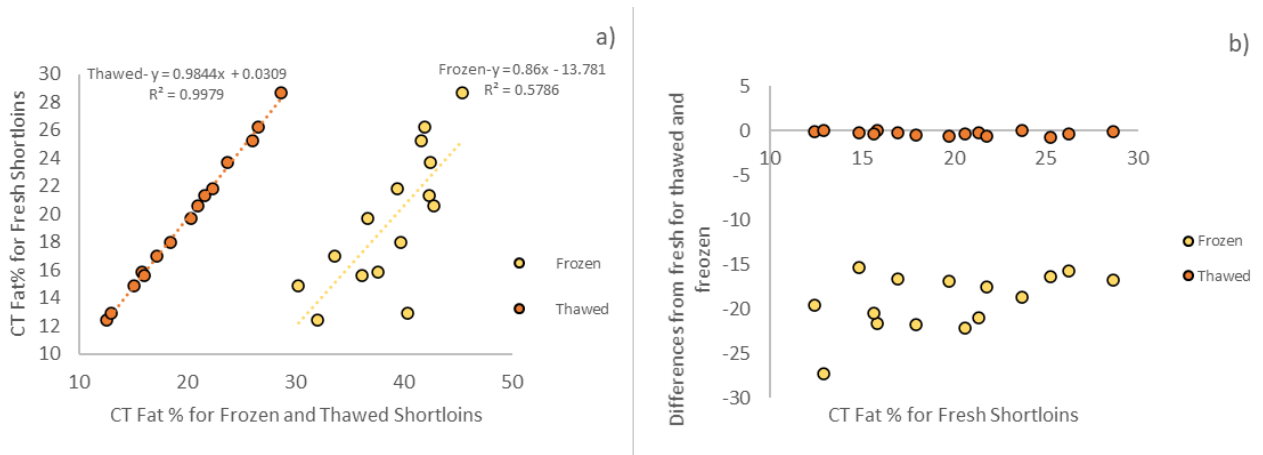


**Figure 27.** Comparison of a) CT Fat % predictions for fresh short-loins versus frozen and thawed short-loins, and b) CT Fat% differences for fresh short-loin values minus frozen or thawed short-loin values versus CT Fat% for fresh short-loins.

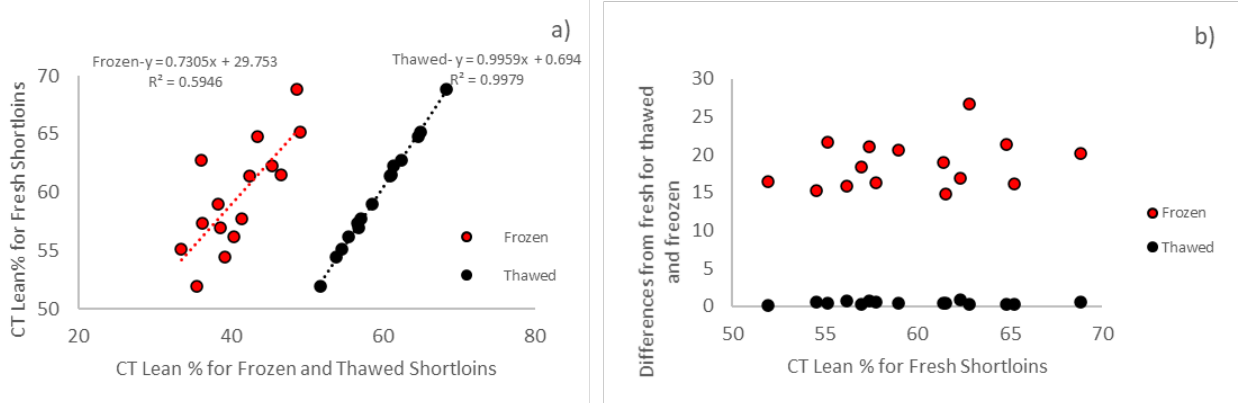


**Figure 17.** Comparison of a) CT Lean % predictions for fresh short-loins versus frozen and thawed short-loins, and b) CT Lean % differences for fresh short-loin values minus frozen or thawed short-loin values versus CT Lean% for fresh short-loins.

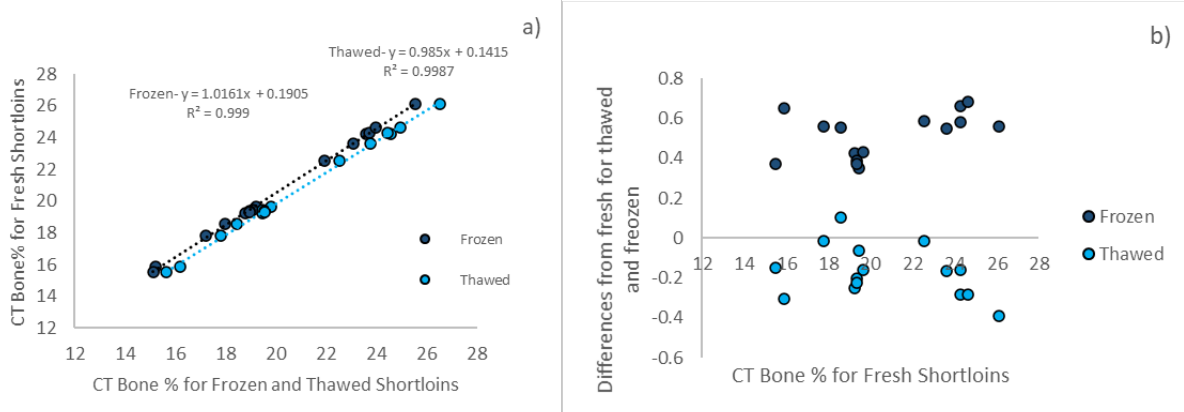


**Figure 29.** Comparison of a) CT Bone % predictions for fresh short-loins versus frozen and thawed short-loins, and b) CT Bone% differences for fresh short-loin values minus frozen or thawed short-loin values versus CT Bone% for fresh short-loins.

### 4.2.3 Voltage

The equations relating the Hounsfield unit values of fat, lean, and bone voxels scanned at either 100kV or 135kV to the equivalent voxels scanned at 120kV are shown in **Figure 30** , and **Figure 31**. In all cases the fit of these equations was excellent, with  $R^2$  values greater than 0.91. Using these equations, the threshold values at 120kV were transformed into their equivalent values at 100kV or 135kV, as reported in **Table 3**.

**Table 3** – Thresholding Parameters used during image analysis of Experiment 2 on images scanned at 100kV and 135kV.

Voltage	Tissue Type	Threshold limit applied
100kV	Bone	214.7335
	Lean	2.5 to 214.7335
	Fat	-250 to 2.5
120kV	Bone	>165
	Lean	2.5 to 165
	Fat	-250 to 2.5
135kV	Bone	149.6669
	Lean	2.5 to 149.6669
	Fat	-250 to 2.5

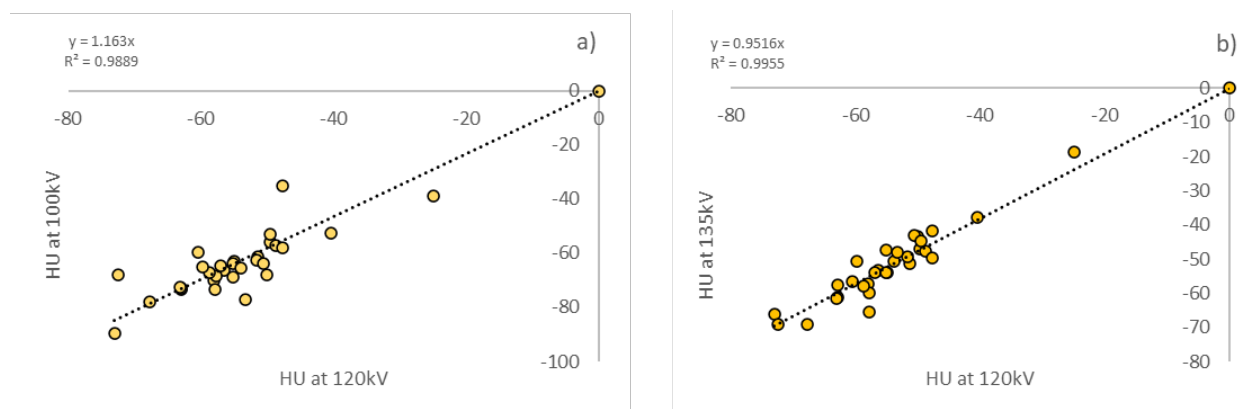


**Figure 30**-Voltage HU Comparisons **a)** HU for Fat at 100kV vs 120kV, **b)** HU for Fat at 135kV vs 120kV.

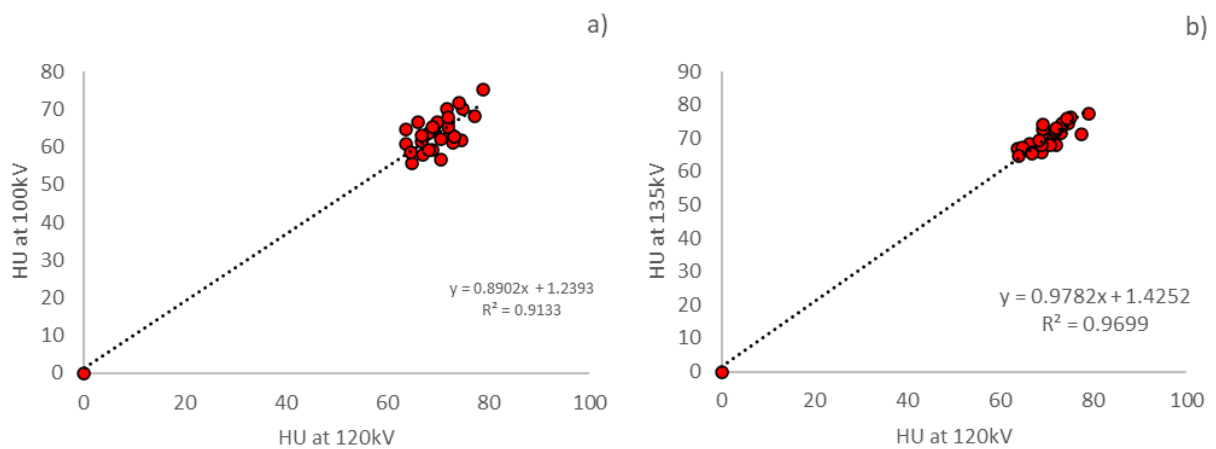


**Figure 18-** Voltage HU Comparisons **a)** HU for Lean at 100kV vs 120kV, **b)** HU for Lean at 135kV vs 120kV.

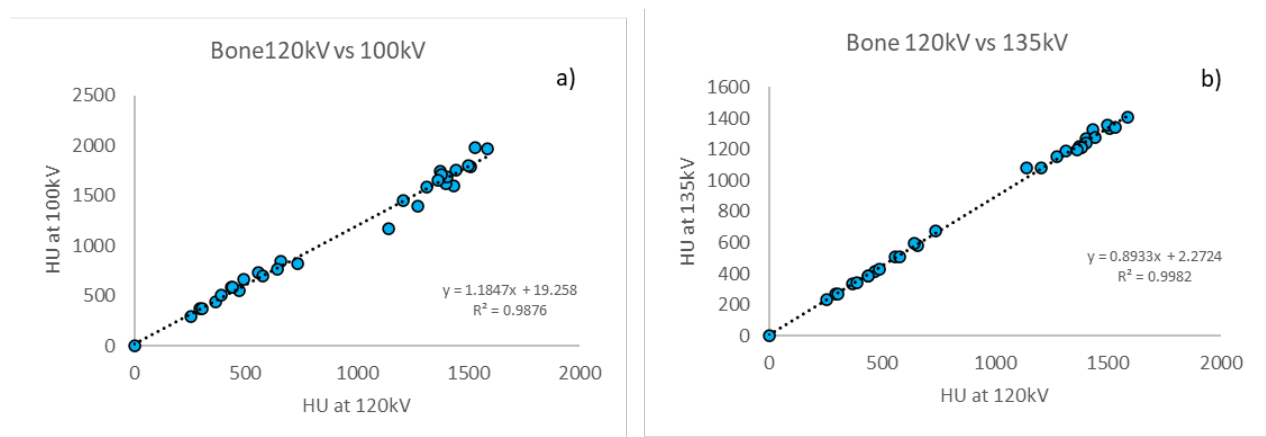


**Figure 32-** Voltage HU comparisons **a)** HU for Bone at 100kV vs 120kV, **b)** HU for Bone at 135kV vs 120kV.

#### 4.2.4 Thresholding Adjustment- fixed density and new thresholds from linear equation

The new threshold parameters reported in **Table 3** were applied to the images captured at 100kV and 135kV, along with a fixed density for each tissue type and the images reanalyzed.

Bone composition values showed the largest correction after applying these threshold adjustments to the 100kV and 135kV scans, in both cases aligning well with the Bone% estimates from the 120kV scans (**Figure 33e** and **f**). Estimates of Lean% also demonstrated better alignment with the Lean% predictions at 120kV after applying the altered threshold adjustment (**Figure 33c** and **d**). Fat showed the least change to values before and after

threshold adjustment but its 100kV and 135kV yield predictions were also the most closely aligned to the 120kV predictions prior to threshold adjustment. (Figure 33a and b).

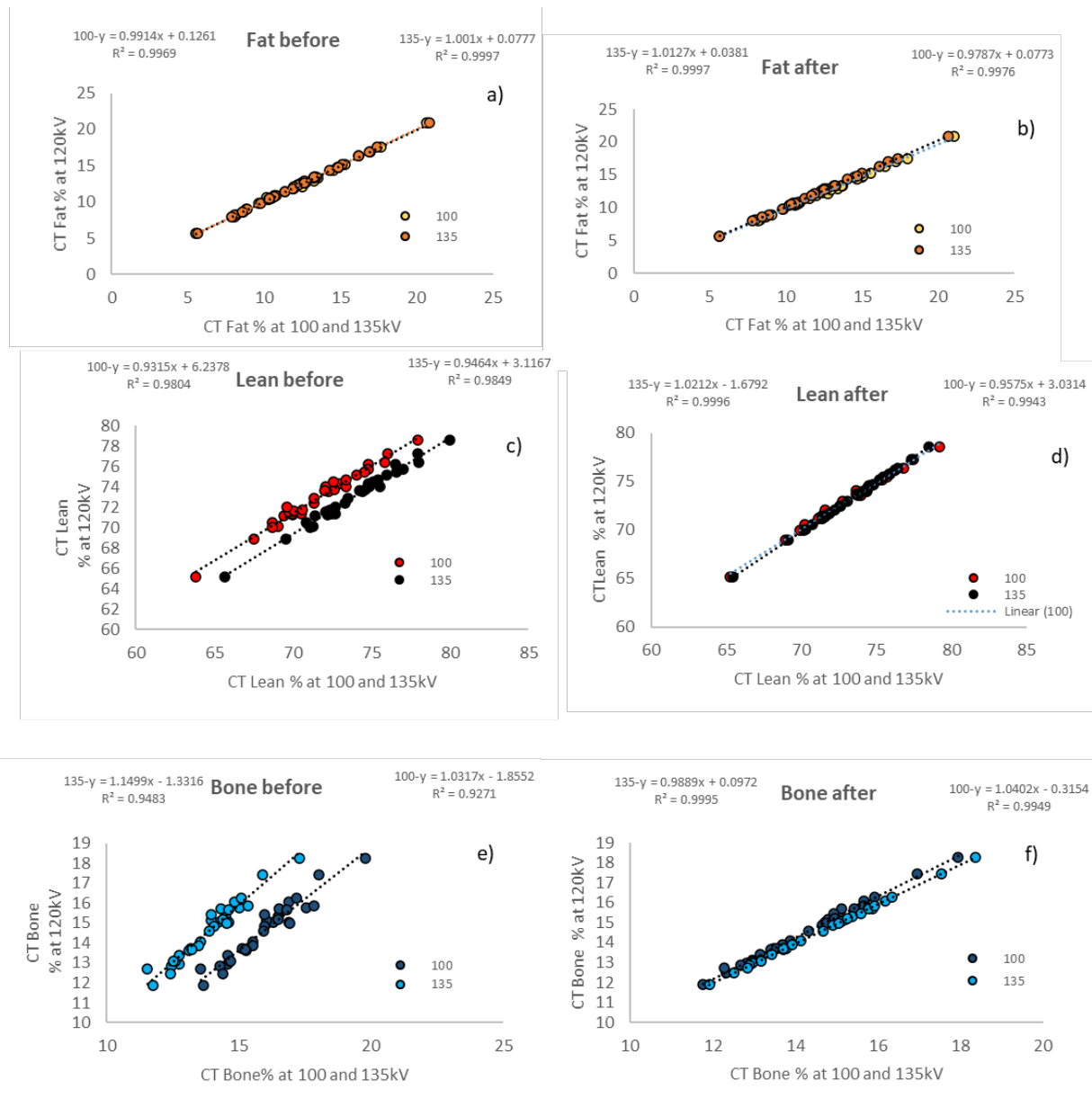


**Figure 33.** CT yield% estimates at 100 and 135kV compared CT yield% estimates at 120kV, before applying the threshold adjustment for a) Fat%, c) Lean%, and e) Bone%, and after applying the threshold adjustment for b) Fat%, d) Lean%, and f) Bone%.

Similar findings are expressed in Figure 34. Both Lean% (Figure 34c and d) and Bone% (Figure 34e and f) at 100kV and 135kV show a substantial decrease in differences from the estimates at 120kV after thresholding with the average differences for Lean%.



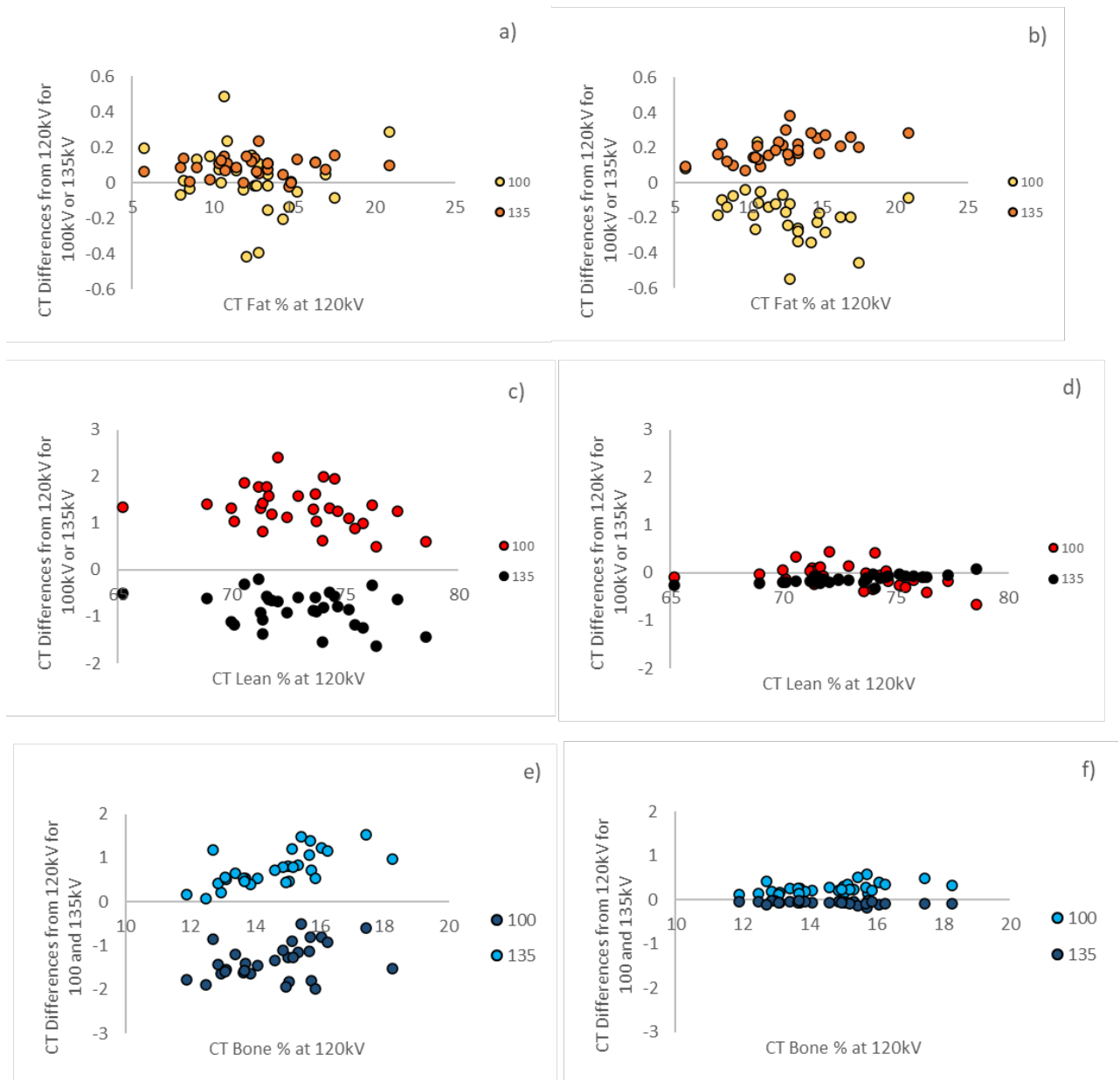


**Figure 34.** The difference between tissue composition estimates measured at 100kV and 135kV from those measured at 120kV before threshold adjustments for a) Fat%, c) Lean%, and e) Bone%, and then after the threshold adjustment had been applied for b) Fat%, d) Lean%, and f) Bone%.

#### 4.2.5 Chemical composition of Beef

In Beef butts Chemical Protein % and CT Lean % were strongly associated, with an  $R^2$  of 0.83 and RMSE of 2.87% (**Figure 35**). The association between Chemical Lipid % and CT Fat % was also strong, with an  $R^2$  of 0.93 and RMSE of 1.10% (**Figure 36**); a slightly stronger association than that seen between Chemical Protein %, and CT Lean %.

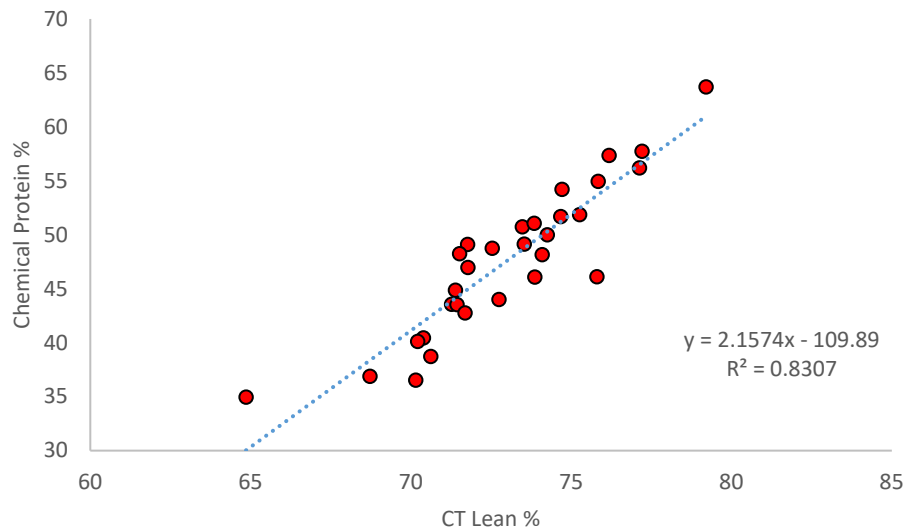


**Figure 195** - CT Lean % vs CT Chemical Protein % in 30 beef butts. Chemical Protein % values represent the mean of 5 sub-samples.

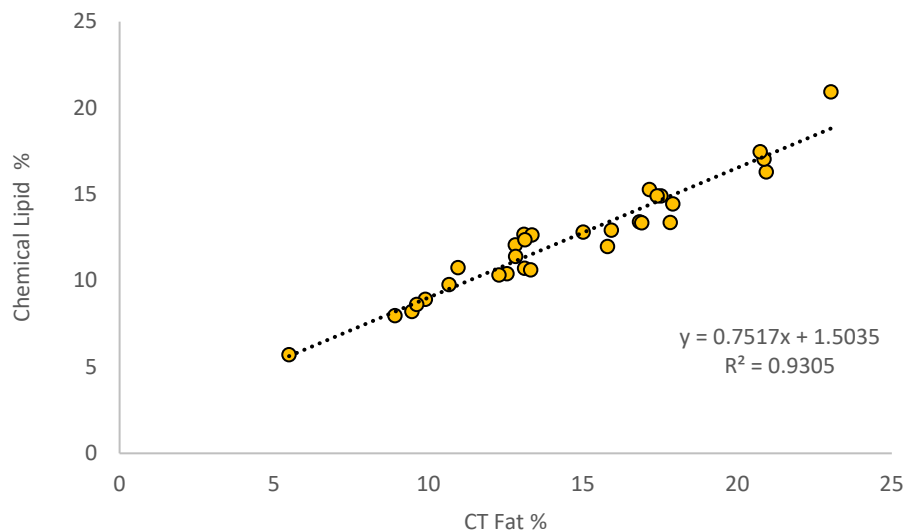


**Figure 36**-CT Fat % vs CT Chemical Lipid % in 30 beef butts. Chemical Lipid % values represent the mean of 5 sub-samples.



#### 4.2.5.1 Sampling variability- Beef

The variation in values across the 5 sub-samples taken within each beef butt were about 50% higher for Chemical Lipid% compared to Chemical Protein%. This is best represented by the higher coefficient of variation for Chemical Lipid %, which is calculated as the standard deviation divided by the mean of the values (**Table 4**). Conversely, the minimum and maximum range of these values was greater for Chemical Protein %, with a range of 19.9% (**Table 3**), compared to Chemical Lipid % variability with a range of 8.14 %.

*Table 4- Minimum, Maximum, Standard Deviation and Coefficient of Variation for the variation between the 5 sub-samples taken within each beef butt to determine Chemical Protein % and Chemical Lipid%. These variation values were calculated within each set of 5 sub-samples, by subtracting the mean of the 5 sub-samples from the individual sample value.*

<b>BEEF</b>	<b>Chemical Protein %</b>	<b>Chemical Lipid %</b>
<b>Min</b>	-11.09	-3.73
<b>Max</b>	8	4.39
<b>STDEV</b>	2.52	1.07
<b>Coeff Var</b>	0.044	0.074

## **4.3 Discussion**

### **4.3.1 Slice Width**

Slice width was found to influence composition estimates, with CT estimates for 5mm slice widths slightly higher for Bone% and slightly less for Fat%, although unchanged for Lean%. It is not immediately clear which slice width delivers the best results, however this does demonstrate the need to standardize this protocol. Future data will test the alignment with chemical composition, however in this study we were able to compare the sum of all components with estimates of carcass weight. In this case the 5mm slice width showed the strongest association, suggesting that it has the most precision for estimating volume. This also aligns with our standardized protocol for scanning nucleus flock lambs, as well as the European position on CT where they have adopted 5mm as the standard slice width for assessing pork composition. Therefore, at this point 5mm will be retained as the optimal width for determining carcass composition in beef carcasses.

### **4.3.2 Voltage**

The effect of voltage varied across tissue types. As was the case in lamb the largest effect was seen in bone, where HU values were markedly lower at 135kV compared to 120kV, while the opposite was seen at the 100kV scanning voltage. The effects on fat and lean were much smaller and opposite in magnitude to the effects on bone. At 100kV the fat and lean voxels were between 5HU and 10HU lower than those at 120kV, and at 135kV there was little difference in voxel values compared to 120kV.

This differential variation in Hounsfield unit value for each tissue type implies that the current method of allocating pixels into Fat, Lean or Bone based on fixed HU thresholds will cause re-allocation of pixels as voltage changes, mainly between bone and lean, causing the overall composition percentages for each tissue type to shift. By amending these thresholds to match the voltage used, we attempted to correct for this error. After reprocessing the images using these adjusted thresholds the estimated carcass composition was found to be more consistent across voltages, although small discrepancies still exist. Future analysis will attempt to correct for this error by referencing components within a commercially available synthetic phantom (XTE CT phantom).

As with the lamb CT methodology, our intention is that no matter what a machine's make and model, and its voltage capabilities, by applying adjustments to a set algorithm we can realign all composition values to those of 120kV, standardizing the CT carcass predictions. However, for the purposes of calibrating other technologies, the CT scanning voltage should always be set at a voltage of 120kV, removing the need for these adjustments.

### **4.3.3 Freeze/thaw effects**

Scanning thawed ribsets and shortloins that had previously been frozen had little observable effect on CT estimates of composition. This implies that when scanning cannot be undertaken soon after slaughter, the carcass or its components can be frozen to guard against meat spoilage, and then defrosted for subsequent scanning. Alternatively, scanning carcass components in a frozen state produced vastly different results, particularly for fat and lean tissues which increased and decreased respectively in their percentage composition due to an associated decrease in average Hounsfield unit values. This clearly demonstrates that carcasses cannot be scanned in a frozen state for the purposes of determining carcass composition or for calibrating other technologies.

### **4.3.4 Chemical Composition**

There were very similar findings for both beef and lamb (see section 3.3.5). As expected, CT Lean % predictions demonstrated a good association with Chemical Protein %, and CT Fat % predictions showed a strong association with Chemical lipid %. These strong associations demonstrate that CT Lean % and CT Fat % can predict chemical protein and fat composition in beef, demonstrating its equivalence to this historical measure of carcass composition.

Chemical analysis for both protein and lipid showed marked sub-sample variation. Despite the rigorous grinding and mixing procedures, residuals of up to 11 protein percentage units from the mean and 4 fat percentage units from the mean were still present between subsamples. This variation in sampling makes calibration of objective measurement tools against chemical analysis an unreliable method when compared to CT. Furthermore, CT has the advantage of being non-destructive.

## **4.4 Conclusions**

These experiments demonstrate the robustness of the CT method to determine non-destructive estimates of carcass composition. This is an essential attribute for CT to act as a calibrating gold standard against which other lean meat yield measurement technologies can be accredited. We have also explored a range of factors that can impact these estimates for both lamb and beef, demonstrating the need to carefully standardize these at the point of scanning. This includes, CT slice width, fresh vs frozen vs thawed cuts and CT voltage at the point of scanning. While adjustments can be made to account for these effects, standardizing the scanning protocol will eliminate this requirement. To ensure the best estimate of carcass composition, and to be consistent with previous studies this standardized protocol should include scanning at CT image slice widths of 5mm, scanning fresh or thawed carcasses, and using a scanning voltage of 120kV.

The industry would benefit from the replacement of the expensive, labour intensive and less reliable method of chemical analysis for carcass composition measurement and training of objective measurement tools. CT is a fabulous alternative, the speed of data turnaround is within minutes for a CT image vs weeks/months for chemical with a significant labour required for whole carcass grinding and subsequent chemical analysis for protein, lipid and ash. With CT there is zero carcass destruction, the carcasses or cuts can be used for further data collection post scanning and in some cases stay within the cold chain and move to saleable cuts, and the immediate repeatability shows no concern for sampling error as chemical analysis has. This is another piece of the puzzle in cementing CT as the new gold standard measure for carcass composition and training/calibration of new and old objective measurement tools.

## 5. The repeatability of CT scanning plastic phantoms

### 5.1 Methodology

#### 5.1.1 Experiment 1- Comparison of Plastic block between different CT devices

A plastic phantom was developed and scanned on 3 different CT scanners. The phantom was made of plastics of 5 different densities. The outside plastics (**Figure 37**) are made from 2 different density plastics, one high density and one low, while the 3 internal rods represented densities that are close to lean and fat. These rods from most to least dense were made from polymethyl methacrylate (PMMA- 1.194 g/cm<sup>2</sup>), Nylon 6 (1.15 g/cm<sup>2</sup>) and polyphenylene ether (PPE- 0.855g/cm<sup>2</sup>). The plastic phantom was scanned on 3 devices with the same setting described in section 3.1 and 4.1. Two devices were located in Western Australia, Murdoch University (MU) and Perth Veterinary Specialists (PVS) were same model described in section 3.1. The third device was located at the University of New England in Armidale, New South Wales, and this device was a Picker PQ 5000 spiral CT scanners. The phantom was scanned at 4 different voltage setting on each device, 80, 100, 120 and 135kV (140kV for the UNE scanner as there was no 135kV setting). The images were analyzed using Image J and the average HU of the internal rods were measured in 10 different images across the length of the scan. These means are presenting in **Table 5** along with the standard deviation.

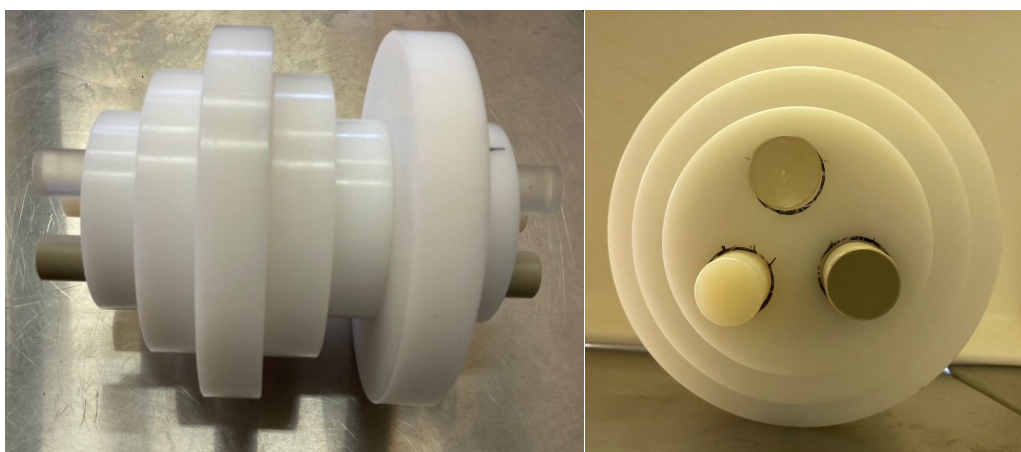


**Figure 37.** The plastic phantom for calibration across different CT devices.

#### 5.1.2 Experiment 2 – Compariosn of the XTE-CT phantom between different CT devices

In a second round of phantom scanning tests, the XTE-CT test piece (**Figure 38**) was scanned a total of 5 times through the two medical CT scanners located in Western Australia, Murdoch University (MU), and Perth Veterinary Specialists (PVS).

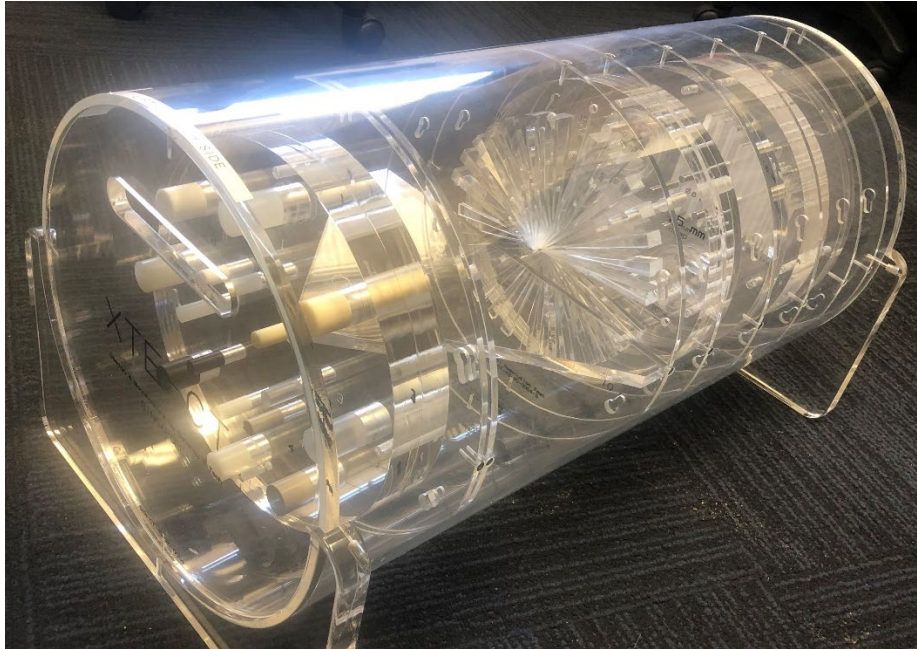


*Figure 38. XTE-CT test piece.*

A section of this test-piece consists of a series of rods inserted into Perspex. These rods are selected to provide a variety of densities in the organic range, with cross-sectional scans captured both within the Perspex where the rods are completely surrounded by Perspex (see right side image in **Figure 39**), and also where they extrude from the Perspex and are therefore surrounded by air (see left side image in **Figure 39**). In this case the average Hu value of the pixels depicting each of the rods was determined. These rods and their corresponding densities included polypropylene ( $0.91 \text{ g/cm}^3$ ), acrylonitrile butadiene styrene ( $1.0 \text{ g/cm}^3$ ), polycarbonate ( $1.1 \text{ g/cm}^3$ ), peek ( $1.3 \text{ g/cm}^3$ ), Delrin ( $1.4 \text{ g/cm}^3$ ), chlorinated PVC ( $1.5 \text{ g/cm}^3$ ), polyvinylidene fluoride ( $1.75 \text{ g/cm}^3$ ), Teflon ( $2.2 \text{ g/cm}^3$ ), and the scattering plate consisted of Perspex ( $1.2 \text{ g/cm}^3$ ). The scans of this section were assessed across each of the 5 repeat scans for both medical CT scanners, enabling quantification of repeatability of these performance indicators. For assessment of the XTE-CT test piece, where quantitative values were available, these were pooled across the 5 scans taken on the two CT medical scanners. The mean, standard deviation, minimum, and maximum values across these 5 scans was then reported for each scanner.

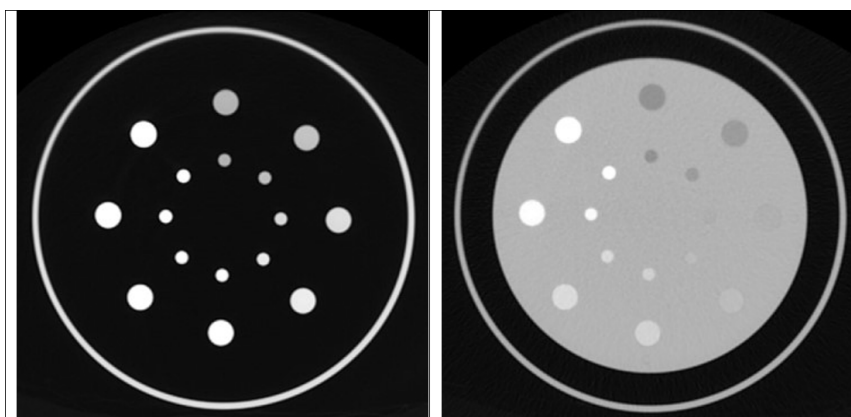


**Figure 39.** The density test showing rods embedded in Perspex (on the right) and rods extending out of Perspex and surrounded by air (on the left).

## 5.2 Results

The mean data for the HU outputs on different devices for different density plastics at multiple voltage settings can be seen in **Table 5**. The HU outputs varied between devices. As the density of the plastics increased the HU unit increased relatively linearly. Scans from PVS at all voltage settings mostly had the lowest HU outputs, while scans from UNE had the highest HU outputs. At 80kV, the difference between devices was the greatest, with the means differing as much as 17.74 HU for PPE, 13.95 for nylon and 13.66 for PMMA. As the voltage increased, the difference of the outputs decreased with 120kV and higher resulting in the smallest difference between devices. For scans at or above 120kV, the sum of the standard deviation of the means between sites was likely greater than the difference of these means. The scans of PPE, nylon, and PMMA acquired from different sections of the phantom were quite consistent irrespective of the depth of the surrounding outer material.

**Table 5.** The Hounsfield units (HU) outputs from different CT devices when measuring plastics of differing densities. Scans were done at 4 different voltage settings, presented as means with standard deviations. \*The 135kV scan at UNE was actually 140kV.

Plastic	Density (g/cm <sup>2</sup> )	Scanner	Voltage (kV)							
			80		100		120		135*	
			Mean HU	STD	Mean HU	STD	Mean HU	STD	Mean HU	STD
<b>PPE</b>	0.855	<b>UNE</b>	-113.72	7.36	-90.62	6.25	-91.52	6.52	-85.80	5.65
		<b>PVS</b>	-131.46	6.06	-107.32	4.17	-100.10	3.75	-96.66	5.25
		<b>MU</b>	-123.06	7.89	-100.51	4.10	-93.47	1.39	-88.24	1.76
<b>Nylon</b>	1.15	<b>UNE</b>	58.93	6.24	75.79	7.39	88.00	4.33	94.38	5.13
		<b>PVS</b>	44.98	3.91	65.63	5.38	76.24	5.60	82.12	5.74
		<b>MU</b>	45.52	3.26	68.46	2.79	80.99	4.23	87.09	3.57
<b>PMMA</b>	1.194	<b>UNE</b>	99.88	5.71	111.56	6.24	121.31	4.83	126.49	4.66
		<b>PVS</b>	88.65	5.15	na		111.71	6.54	116.79	6.13
		<b>MU</b>	86.22	3.00	103.27	7.19	113.17	4.51	118.47	4.99

The density test for the XTE-CT test piece demonstrated excellent alignment of values between scanners irrespective of whether these materials were scanned from sections surrounded by air (**Figure 40**), or by Perspex (**Figure 41**). However, as was the case for the Murdoch phantom scans (**Table 6**), the absolute values returned for the scans of these materials differed slightly. This was evident from the “site differences” reported in **Table 6**, with the values reported for materials surrounded by Perspex most relevant to the carcass scenario as in this case tissues are scanned in mixtures of bone, muscle, and fat. While these values varied by as much as 7HU, the materials with densities similar to fat and lean, ABS, Polycarbonate and Peek, varied least with differences of between 2HU to 4HU.

One comparison where differences between sites were particularly marked were for the higher density materials such as Delrin, PVC, PVDF, and Teflon when scanned surrounded by air. In this case site differences were 18.9, 17.4, 23.7, and 26.8HU for these materials (**Table 6**).



**Table 6.** The Hounsfield units (HU) outputs from different CT devices when measuring plastics of differing densities surrounded by air or by perspex. Scans were done at Murdoch University and Perth Veterinary Services. Values are mean, minimum, maximum and standard deviations of 5 scans of the plastic sections, as well as the average standard deviation of the pixel values within these sections. The site difference represents the difference between the mean value at each site for each material.

		Murdoch University					Perth Veterinary Services					Site Difference
		Mean	Min	Max	STDEV	Ave Std of pixels	Mean	Min	Max	STDEV	Ave Std of pixels	
Polypropylene	In Air	-134	-141	-120	8.71	7.42	-140	-142	-138	1.93	7.13	5.92
ABS	In Air	-60.	-70.	-53.	6.99	6.65	-67.	-69.	-66.	1.37	6.17	7.57
Polycarbonate	In Air	75.0	62.8	87.2	10.4	6.30	66.5	64.2	69.4	2.12	6.57	8.51
Peek	In Air	155.	143.	165.	7.93	5.95	148.	144.	154.	4.69	6.43	6.69
Delrin	In Air	304.	296.	316.	7.58	6.34	285.	279.	294.	7.22	7.08	18.9
PVC	In Air	365.	353.	374.	10.6	7.03	348.	344.	351.	3.34	8.25	17.4
PVDF	In Air	613.	587.	643.	26.4	12.3	589.	585.	592.	3.59	12.5	23.7
Teflon	In Air	927.	891.	976.	44.3	20.6	900.	889.	909.	9.27	16.8	26.8
Polypropylene	In perspex	-93.	-100	-80.	7.93	12.9	-101	-102	-98.	1.83	9.77	7.07
ABS	In perspex	-28.	-38.	-15.	8.40	11.4	-30.	-34.	-26.	3.23	9.21	2.43
Polycarbonate	In perspex	97.3	82.8	109.	9.75	10.8	101.	97.3	104.	3.68	8.94	-4.0
Peek	In perspex	176.	160.	183.	9.76	9.85	178.	174.	185.	5.09	8.96	-2.1
Delrin	In perspex	307.	299.	313.	5.13	11.5	308.	299.	317.	9.16	9.36	-1.1
PVC	In perspex	366.	360.	373.	4.84	11.8	370.	366.	375.	3.96	8.46	-3.6
PVDF	In perspex	596.	572.	619.	17.9	14.3	598.	591.	607.	6.92	11.8	-2.0
Teflon	In perspex	891.	848.	946.	37.1	16.0	897.	879.	912.	14.8	13.7	-6.4
Perspex		113.	103.	124.	6.96	13.4	125.	118.	130.	4.08	10.3	-11.

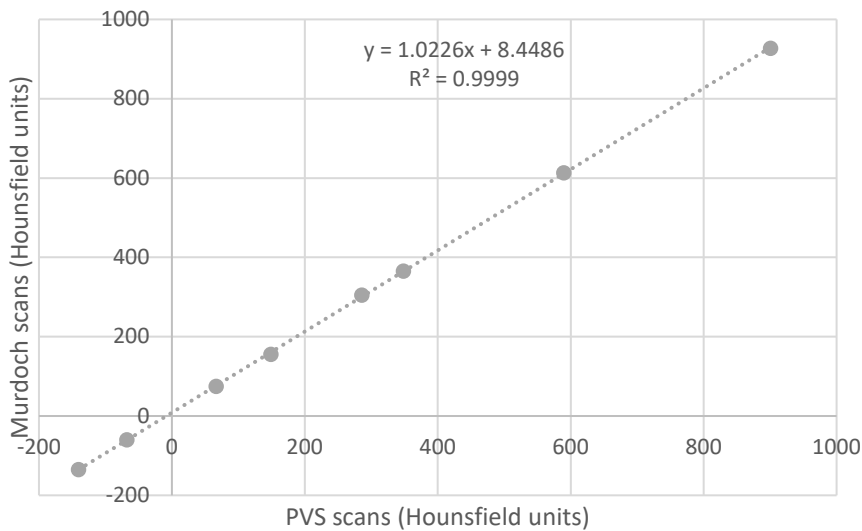


**Figure 40.** Hounsfield unit values for different density materials in the XTE-CT test piece, scanned at Murdoch University versus values scanned at Perth Veterinary Services (PVS). In this case materials are surrounded by air.

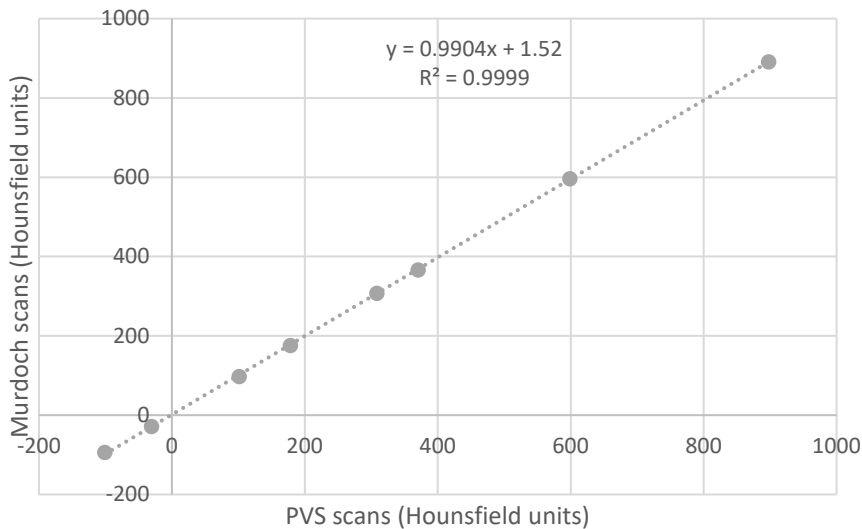


**Figure 41.** Hounsfield unit values for different density materials in the XTE-CT test piece, scanned at Murdoch University versus values scanned at Perth Veterinary Services (PVS). In this case materials are surrounded by perspex.

### 5.3 Discussion

Although the HU outputs between devices varied, when scanned at the optimal voltage setting of 120kV these differences were minimized and the differences between devices was small. When comparing the same device model (MU and PVS) there were still variations in

the outputs which were of similar magnitude when compared to a different device model. Thus, it is likely that simple site differences account for most of the variation in HU scan values, as opposed to company and model differences between CT scanners. All CT devices returned the expected differences in HU values for the variety of plastics scanned, given their known densities and attenuation coefficients. These relative differences between materials were highly consistent between devices, as demonstrated by the excellent association in scanned values between sites (see **Table 6**). Given this consistency, it suggests that small differences in scan values between sites may be adjusted for by a linear shift relative to a phantom standard. This approach may also be suitable for adjusting scanning image sets acquired at different voltages. The HU outputs increased with increasing voltage, in many cases by varying amounts. Hence the adjustment would likely require both a slope and intercept adjustment of HU values to align data sets. However, the impact that any adjustment has on the lean/fat thresholds needs to be determined, and potentially adjusted for when separating tissue types based upon these thresholds.

Much of this variation due to voltage would be avoided by simply standardizing the voltage settings for measuring carcasses. As such, from the results of this study we would recommend that a scan voltage of 120kV is standardized, as this returns values that are most repeatable, and vary least between devices.

## 6. References

Gundersen, H. J. G. & Jensen, E. 1987. The efficiency of systematic sampling in stereology and its prediction. *Journal of microscopy*, 147, 229-263.

Mull, R. T. 1984. Mass estimates by computed tomography: Physical density from CT numbers. *American Journal of Roentgenology*, 143, 1101-1104.

Williams, A., Anderson, F., Siddell, J., Pethick, D., Hocking, E. J. & Gardner, G. 2017. Predicting lamb carcass composition from carcass weight and GR tissue depth. 63rd International Congress of Meat Science and Technology. Cork, Ireland, 729-732.